Electronic Supplementary Information

Recognition and Protection of Glycosphingolipids by Synthetic Nanoparticle Receptors

Roshan W. Gunasekara and Yan Zhao*

Department of Chemistry, Iowa State University, Ames, Iowa 50011-3111, USA

Table of Contents

General Method

All the glycosphingolipids in this study were bought from Matreya LLC. All other reagents and solvents were of ACS certified grade or higher and were used as received from commercial suppliers. Routine ^{1}H and ^{13}C NMR spectra were recorded on a Bruker DRX-400, on a Bruker AV II 600 or on a Varian VXR-400 spectrometer. ESI-MS mass was recorded on Shimadzu LCMS-2010 mass spectrometer. Dynamic light scattering (DLS) data were recorded at 25 °C using PDDLS/ CoolBatch 90T with PD2000DLS instrument. Isothermal titration calorimetry (ITC) was performed using a MicroCal VP-ITC Microcalorimeter with Origin 7 software and VPViewer2000 (GE Healthcare, Northampton, MA). All the glycosphingolipids were bought from Matreya LLC. Amplex red galactose/ galactose oxidase assay kit (catalog number: A22179) was bought from Thermo Fisher Scientific.

Abbreviation

HEPES: 4-(2-hydroxyethyl)-1-piperazineethanesulfonic acid; POPC: 1-palmitoyl-2-oleoyl-sn-glycero-3-phosphocholine; POPG: 1-palmitoyl-2-oleoyl-sn-glycero-3-[phospho-rac-(1-glycerol)] sodium salt.

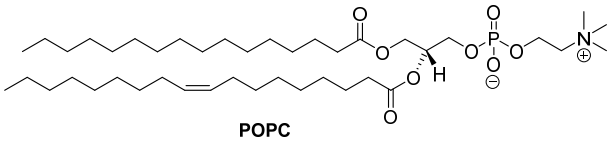

POPC

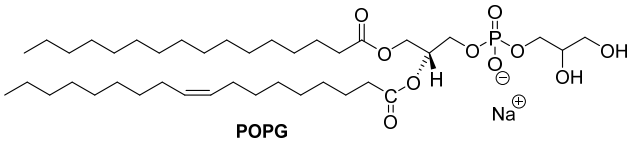

POPG

Scheme S1

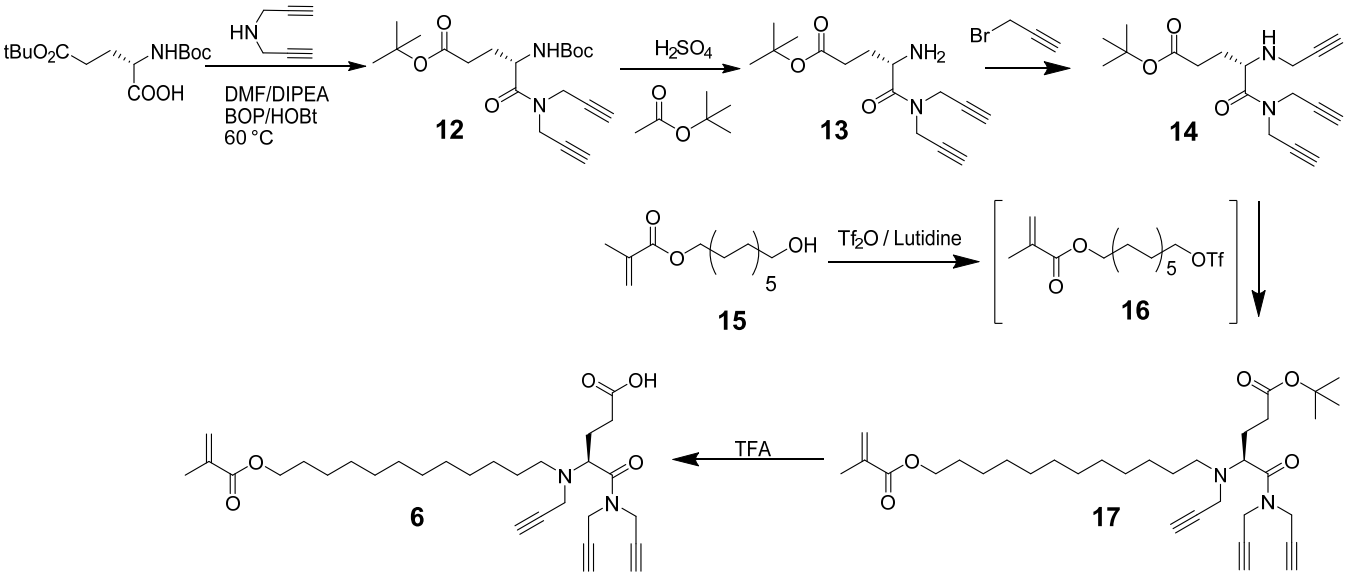

Syntheses

Compounds **7**[1] and **15**[2] were synthesized following reported procedures.

Compound 12. N-Boc-L-glutamic acid gamma *t*-butyl ester (1.0 g, 3.3 mmol), dipropargylamine (0.31 g, 3.3 mmol), benzotriazol-1-yloxytris(dimethylamino)phosphoniumhexafluorophosphate (BOP, 1.46 g, 3.3 mmol), 1-hydroxybenzotriazole hydrate (HOBt, 0.446 g, 3.3 mmol), and N,N-diisopropylethyl-amine (DIPEA, 0.87 mL, 5.00 mmol) were dissolved in THF (20 mL). The reaction mixture was stirred for 4 h in a microwave reactor at 50 °C (150 W). After cooled down to room temperature, the solvent was removed *in vacuo*. The residue was purified by column chromatography over silica gel with 6:1 hexane/ethyl acetate as the eluent to give a pale yellow liquid (1.19 g, 96%). ^{1}H NMR (400 MHz, $CDCl_3$, δ): 5.29 (d, *J* = 8.8 Hz, 1H), 4.69 (td, *J* = 9.4, 3.7 Hz, 1H), 4.62–4.10 (m, 4H), 2.32 (m, 3H), 2.24 (t, *J* = 2.5 Hz, 1H), 2.06 (m, 1H), 1.70 (m, *J* = 17.3, 9.0, 4.8 Hz, 1H), 1.63 (s, 1H), 1.44 (d, *J* =

[1] Gunasekara, R. W.; Zhao, Y., *J. Am. Chem. Soc.* **2017,** *139*, 829-835.

[2] Awino, J. K.; Zhao, Y., *J. Am. Chem. Soc.* **2013,** *135*, 12552-12555.

10.3 Hz, 18H). ^{13}C NMR (100 MHz, $CDCl_3$, δ): 172.1, 171.5, 155.4, 80.6, 79.7, 77.8, 77.5, 77.2, 73.5, 72.5, 49.73, 36.1, 34.1, 30.8, 28.4, 28.3, 28.1. ESI-MS (*m/z*): $[M+H]^+$ cacld for $C_{20}H_{31}N_2O_5$, 379.2155; found, 379.2144.

Compound 13. Compound **12** (1.0 g, 2.64 mmol) and conc. H_2SO_4 (0.052 g, 0.53 mmol) were dissolved in *tert*-butyl acetate (20 mL). The reaction mixture was stirred for 20 h at room temperature, neutralized with sat. $NaHCO_3$, and extracted with ethyl acetate (4 × 10 mL). The combined organic phase was dried with anhydrous $MgSO_4$ and concentrated by rotary evaporation. The residue was purified by column chromatography over silica gel with 10:1 dichloromethane/methanol as the eluent to give a pale yellow liquid (0.521 g, 71%). ^{1}H NMR (400 MHz, $CDCl_3$, δ): 4.45–4.02 (m, 4H), 3.63 (dt, *J* = 9.5, 4.6 Hz, 1H), 2.44 (ddt, *J* = 16.4, 7.4, 3.7 Hz, 1H), 2.21 (m, 3H), 1.84 (tdd, *J* = 13.8, 7.1, 4.1 Hz, 1H), 1.65 – 1.11 (m, 12H).

Compound 14. Compound **13** (0.5 g, 1.8 mmol), propargyl bromide (0.21 g, 1.8 mmol), and sodium bicarbonate (0.30 g, 3.6 mmol) were mixed in acetonitrile (10 mL). The reaction mixture was stirred at 40 °C for 12 h, cooled down to room temperature. After the solid was removed by suction filtration, the solvent was removed *in vacuo*. The residue was purified by column chromatography over silica gel with 6:1 hexane/ethyl acetate as the eluent to give a pale yellow liquid (0.53 g, 94%). ^{1}H NMR (400 MHz, $CDCl_3$, δ): 4.57–4.20 (m, 4H), 3.69 (m, 1H), 3.31 (m, 2H), 2.57 (m, *J* = 12.5, 8.9, 4.5 Hz, 1H), 2.45 – 2.07 (m, 5H), 1.90 (qd, *J* = 10.0, 9.5, 3.8 Hz, 1H), 1.44 (s, 10H). ^{13}C NMR (100 MHz, $CDCl_3$, δ): 174.4, 172.2 77.2, 76.8, 73.1, 72.4, 71.6, 56.5, 37.3, 35.67, 34.2, 31.08, 28.6, 28.1. ESI-MS (*m/z*): $[M+H]^+$ cacld for $C_{18}H_{25}N_2O_3$, 317.4010; found, 317.4051.

Compound 17. Triflic anhydride (0.35 mL, 2.1 mmol) and 2,6-lutidine (0.24 mL, 2.1 mmol) were added to 10 mL of dry dichloromethane cooled at -20 °C. The cooling bath was removed and compound **15** (432 mg, 1.6 mmol) in CH_2Cl_2 (5 mL) was added dropwise to the stirred solution. After 90 min, the reaction mixture was diluted with CH_2Cl_2 (5 mL). The organic layer was washed with

water (3 × 10 mL), dried with anhydrous magnesium sulfate, filtered, and concentrated by rotary evaporation to give the triflate as a reddish oil (compound **16**). The oil was dissolved in 2,6-lutidine (0.24 mL, 2.1 mmol), to which compound **14** (0.506 g, 1.6 mmol) in dry THF (10 mL) was added dropwise. After being stirred at room temperature overnight, the reaction mixture was concentrated by rotary evaporation and the residue was purified by column chromatography over silica gel using 1: 50 methanol/CH_2Cl_2 as eluent to afford a pale yellow oil (718 mg, 79%). ^{1}H NMR (400 MHz, CD_3OD, δ): 6.12 (s, 1H), 5.65 (p, *J* = 1.7 Hz, 1H), 4.82 (d, *J* = 2.5 Hz, 1H), 4.43 (dd, *J* = 2.5 Hz, 2H), 4.27–4.11 (m, 3H), 3.92 (dd, *J* = 8.9, 4.4 Hz, 1H), 3.49 (m, 2H), 3.35 (p, *J* = 1.7 Hz, 3H), 2.80 (t, *J* = 2.5 Hz, 1H), 2.67 (m, 3H), 2.55 (dt, *J* =, 6.7 Hz, 1H), 2.33 (m, 1H), 2.25–1.85 (m, 7H), 1.72 (p, *J* = 6.7 Hz, 3H), 1.42 (m, 22H). ^{13}C NMR (100 MHz, CD_3OD, δ): 172.7, 171.3, 167.5, 136.5, 124.6, 80.3, 79.7, 79.0, 78.1, 77.8, 73.3, 73.1, 73.0, 72.2, 70.6, 70.2, 64.6, 61.3, 49.0, 48.1, 47.9, 47.8, 47.6, 47.5, 47.3, 47.2, 38.8, 36.2, 35.8, 34.1, 34.0, 31.9, 31.6, 29.4, 29.4, 29.3, 29.3, 29.3, 29.3, 29.2, 29.0, 28.3, 27.1, 27.0, 27.0, 26.9, 25.9, 25.7, 24.3, 24.1, 21.2, 19.9, 17.1. ESI-HRMS (*m/z*): $[M+H]^+$ calcd for $C_{34}H_{53}N_2O_5$, 569.3949; found, 569.3951.

Compound 6. Compound **17** (0.2 g, 0.35 mmol) and trifluoroacetic acid (0.20 g, 1.75 mmol) were dissolved in dichloromethane (10 mL). The reaction mixture was stirred at room temperature for 20 h before the solvent was removed by rotary evaporation. The residue was mixed with an excess of sodium bicarbonate (0.35 g, 4.2 mmol) in methanol (10 mL). After being stirred at room temperature overnight, the reaction mixture was concentrated by rotary evaporation and the residue was purified by column chromatography over silica gel using 1: 10 methanol/CH_2Cl_2 as eluent to afford a pale yellow oil (172 mg, 92%). ^{1}H NMR (400 MHz, CD_3OD, δ): 6.08 (s, 1H), 5.61 (s, 1H), 4.72 (t, 1H), 4.61–4.26 (m, 4H), 4.15 (q, *J* = 6.9 Hz, 4H), 3.53–3.25 (m, 5H), 2.97 (d, *J* = 3.0 Hz, 1H), 2.42 (m, 2H), 2.27 (m,1H), 1.93 (s, 3H), 1.82 (t, *J* = 18.6, 9.2 Hz, 2H), 1.73–1.50 (m, 6H), 1.50–1.15 (m, 18H). ^{13}C NMR (100 MHz, CD_3OD, δ): 173.9, 167.5, 167.1, 159.8, 136.5, 124.5, 79.9, 76.7, 74.7, 73.0, 71.7,

70.8, 69.4, 64.5, 61.9, 52.5, 48.2, 48.0, 47.8, 47.6, 47.6, 47.4, 47.4, 47.2, 46.9, 39.9, 36.5, 34.9, 34.8, 29.4, 29.3, 29.3, 29.2, 29.2, 29.0, 28.9, 28.6, 28.3, 28.1, 28.0, 26.3, 26.1, 25.9, 25.6, 24.1, 23.0, 22.9, 21.6, 17.0. ESI-HRMS (*m/z*): $[M+H]^+$ calcd for $C_{30}H_{45}N_2O_5$, 513.3323; found, 513.3332.

Determination of Critical Micelle Concentration (CMC) of compound 6

Determination of CMC followed reported literature procedures.[3] Surfactant **6** (9.73 mg, 0.02 mmol) was dissolved in 1.0 mL of an aqueous solution of pyrene (1.0×10^{-7} M). To 17 separate vials, 140, 80, 60, 40, 36, 32, 28, 24, 18, 16, 14, 12, 10, 8, 6, 4, and 2 μL of the above stock solution were added. Millipore water was added to make the total volume of each sample 2 mL. Fluorescence spectra were recorded with the excitation wavelength at 332 nm. The final results were based on duplicate experiments with separately prepared solutions.

Synthesis of MINPs.

MINPs were synthesized according to previously reported procedures.[1] A solution of 6-vinylbenzoxaborole in methanol (10 μL of a 6.4 mg/mL, 0.00040 mmol) was added to the hydrogenated glycosphingolipid in methanol (10 μL of 32.36 mg/mL, 0.0004 mmol) in a vial containing methanol (5 mL). After the mixture was stirred for 6 h at room temperature, methanol was removed *in vacuo*. A micellar solution of compound **6** (0.03 mmol), compound **7** (0.02 mmol), divinylbenzene (DVB, 2.8 μL, 0.02 mmol), and 2,2-dimethoxy-2-phenylacetophenone (DMPA,10 μL of a 12.8 mg/mL solution in DMSO, 0.0005 mmol) in H_2O (2.0 mL) was added to the sugar–boronate complex. The mixture was subjected to ultrasonication for 10 min before $CuCl_2$ (10 μL of a 6.7 mg/mL solution in H_2O, 0.0005 mmol) and sodium ascorbate (10 μL of a 99 mg/mL solution in H_2O, 0.005 mmol) were added. After the reaction mixture was stirred slowly at room temperature for 12 h, the reaction mixture was transferred into a glass vial, purged with nitrogen for 15 min, sealed with a rubber

[3] Zhang, S.; Zhao, Y. *J. Am. Chem. Soc*. **2010**, *132*, 10642-10644.

stopper, and irradiated in a Rayonet reactor for 8 h. Compound **3** (10.6 mg, 0.04 mmol), $CuCl_2$ (10 μL of a 6.7 mg/mL solution in H_2O, 0.0005 mmol), and sodium ascorbate (10 μL of a 99 mg/mL solution in H_2O, 0.005 mmol) were added. After being stirred for another 6 h at room temperature, the reaction mixture was poured into acetone (8 mL). The precipitate collected by centrifugation was washed with a mixture of acetone/water (5 mL/1 mL), and methanol/acetic acid (5 mL/0.1 mL) for three times and finally with acetone (1 × 5 mL) to neutral before being dried in air to afford the final MINP as an off-white powder (~80% yield).

Liposome preparation.

A chloroform solution of POPC (1-palmitoyl-2-oleoyl-*sn*-glycero-3-phosphocholine) was placed in a 10 mL test tube and dried under a stream of nitrogen for 10 min. The residue was dried further under high vacuum overnight to obtain a thin lipid film. A solution of HEPES buffer (1.0 mL, pH = 7.4) with kerasin (**1**) was added to the test tube containing thin lipid film. Rehydration of the lipid was allowed to continue for 90 min with frequent vortexing at 4 °C. The lipid suspensions of the resulting multilamellar vesicles were subjected to ten freeze–thaw cycles. The resulting mixture was then extruded twenty-nine times through a polycarbonate filter (diameter = 19 mm, pore diameters of 30 nm) at room temperature using an Avanti Mini-Extruder to produce the desired large unilamellar vesicles (LUVs). Each LUV was diluted in HEPES to a lipid concentration of 15–25 μM and their size was analyzed by DLS. Intensity data from each sample were collected in five replicates and analyzed by the Precision Deconvolve software.

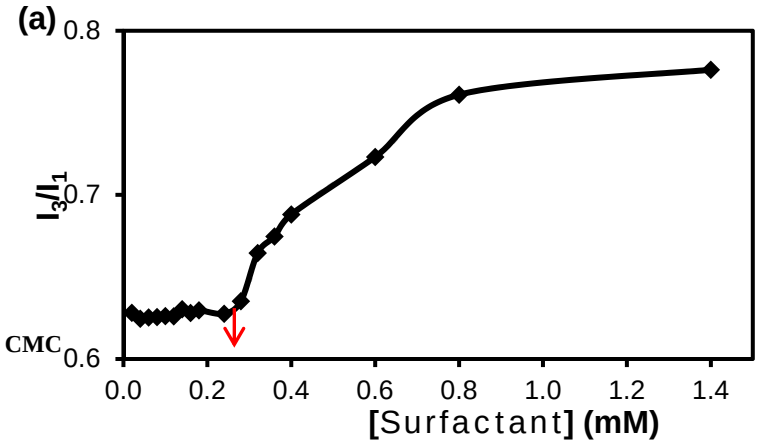

Figure S1. Pyrene I_3/I_1 ratio as a function of [**6**]. [pyrene] = 0.1 μM. The five vibronic bands of pyrene respond to environmental polarity differently. The intensity ratio between the third (~384 nm) and the first band (~372 nm) is particularly sensitive to environmental changes.

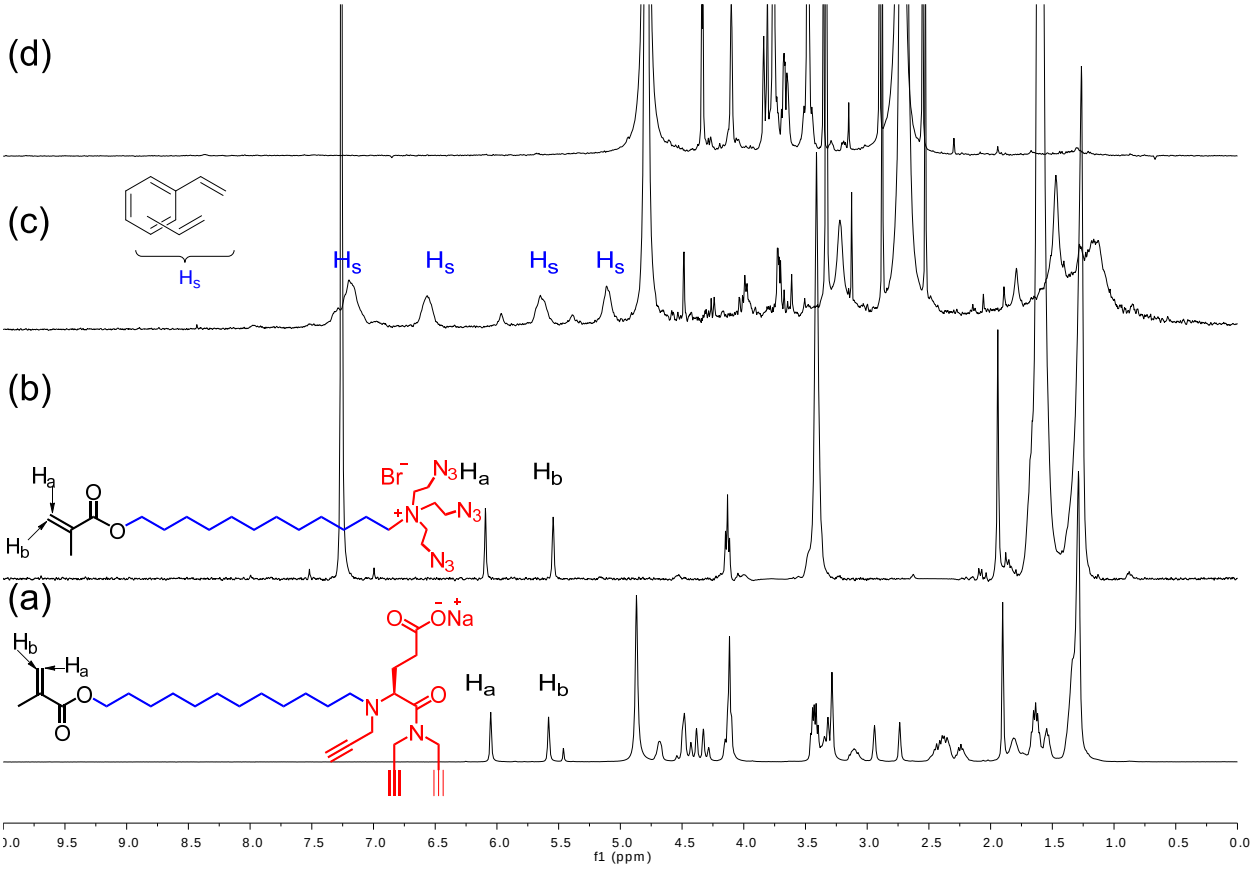

Figure S2. ^{1}H NMR spectra of (a) Compound **6** in CD_3OD, (b) Compound **7** in $CDCl_3$, (c) alkynyl-SCM in D_2O, and (d) MINP(**1**) in D_2O at 298 K.

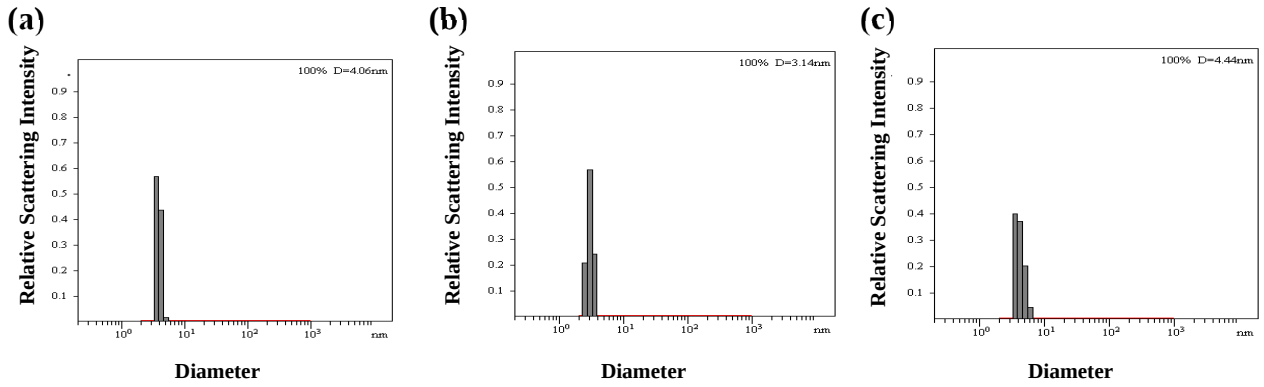

Figure S3. Distribution of the hydrodynamic diameters of the nanoparticles in water as determined by DLS for the synthesis of MINP(**1**) (a) alkynyl-SCM, (b) core-cross-linked-SCM, and (c) surface-functionalized MINP(**1**) after purification.

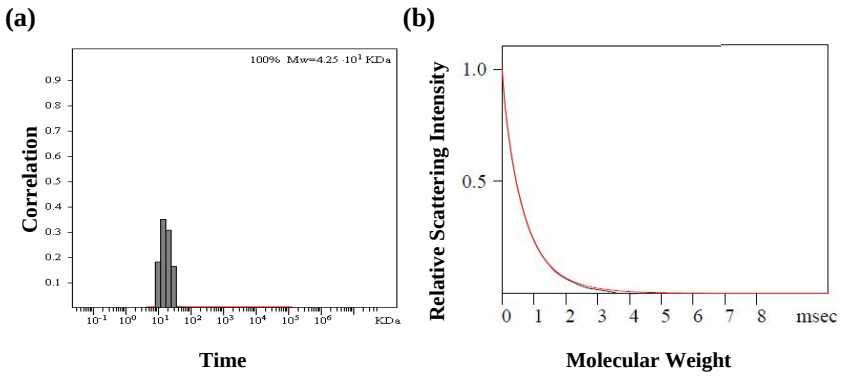

Figure S4. The correlation curve and the distribution of the molecular weight for MINP(**1**) from the DLS. The PRECISION DECONVOLVE program assumes the intensity of scattering is proportional to the mass of the particle squared. If each unit of building block for the MINP(**1**) is assumed to contain 0.6 molecules of Compound **6** (MW = 535 g/mol), 0.4 molecules of compound **7** (MW = 558 g/mol), 0.6 molecules of compound **9** (MW = 264 g/mol), one molecule of DVB (MW = 130 g/mol), and 0.02 molecules of 6-vinylbenzoxaborole (MW = 160 g/mol), the molecular weight of MINP(**1**) translates to 51 [= 42500 / (0.6×535 + 0.4×558 + 0.6×264 + 130 + 0.02×160)] of such units.

System

Temperature (°C):	25.0	**Zeta Runs:**	10
Count Rate (kcps):	116.7	**Measurement Position (mm):**	4.50
Cell Description:	Zeta dip cell	**Attenuator:**	6

Results

			Mean (mV)	**Area (%)**	**St Dev (mV)**
Zeta Potential (mV):	-34.6	**Peak 1:**	-34.6	100.0	10.8
Zeta Deviation (mV):	10.8	**Peak 2:**	0.00	0.0	0.00
Conductivity (mS/cm):	0.353	**Peak 3:**	0.00	0.0	0.00
Result quality :	Good				

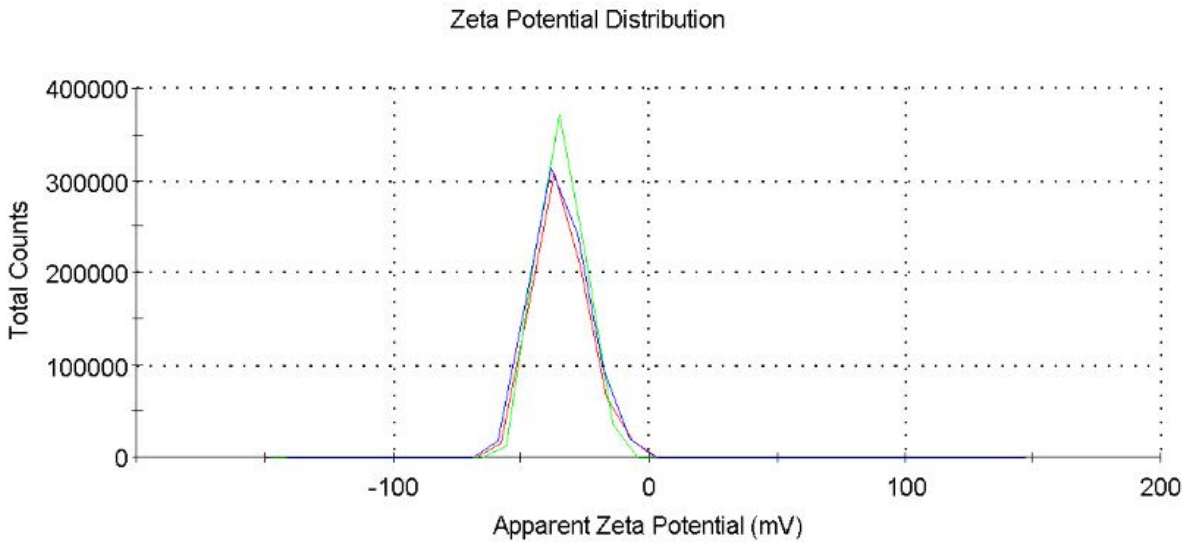

Figure S5. Zeta potential for MINP(**1**) in H_2O measured at 298 K.

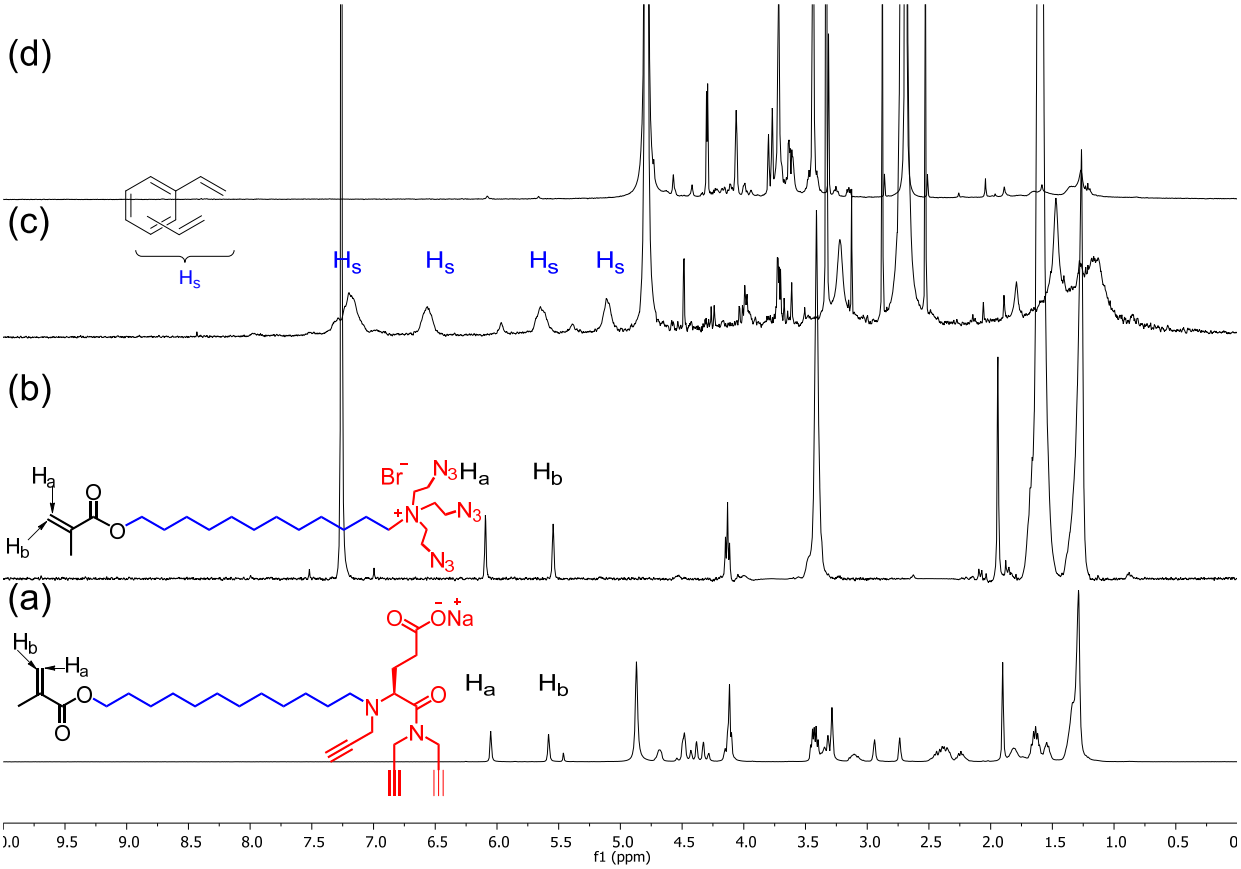

Figure S6. ^{1}H NMR spectra of (a) Compound **6** in CD_3OD, (b) Compound **7** in $CDCl_3$, (c) alkynyl-SCM in D_2O, and (d) MINP(**2**) in D_2O at 298 K.

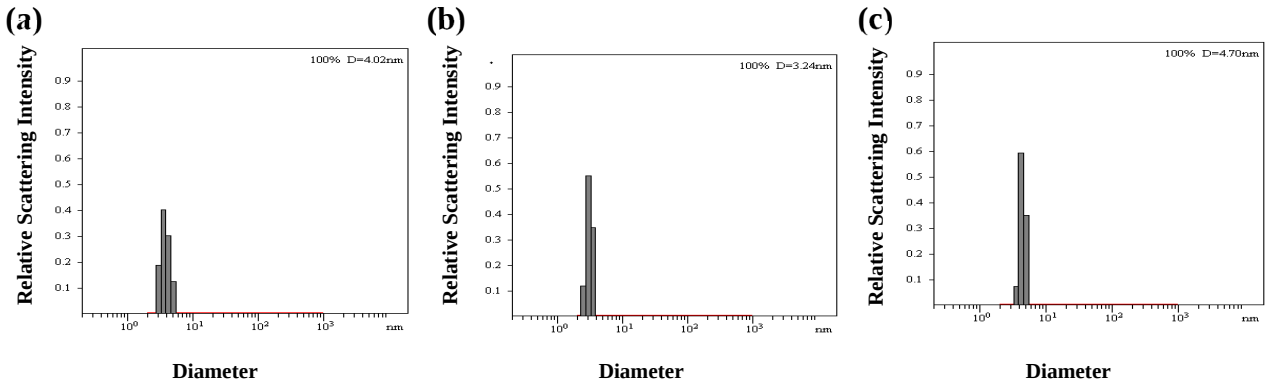

Figure S7. Distribution of the hydrodynamic diameters of the nanoparticles in water as determined by DLS for the synthesis of MINP(**2**) (a) alkynyl-SCM, (b) core-cross-linked-SCM, and (c) surface-functionalized MINP(**2**) after purification.

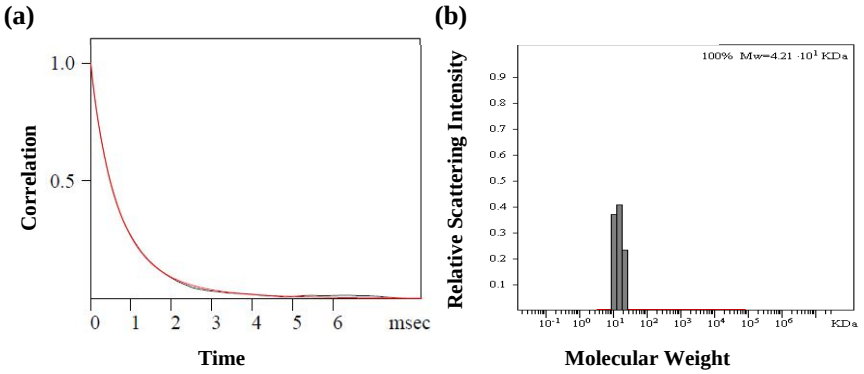

Figure S8. The correlation curve and the distribution of the molecular weight for MINP(**2**) from the DLS. The PRECISION DECONVOLVE program assumes the intensity of scattering is proportional to the mass of the particle squared. If each unit of building block for the MINP(**1**) is assumed to contain 0.6 molecules of Compound **6** (MW = 535 g/mol), 0.4 molecules of compound **7** (MW = 558 g/mol), 0.6 molecules of compound **9** (MW = 264 g/mol), one molecule of DVB (MW = 130 g/mol), and 0.02 molecules of 6-vinylbenzoxaborole (MW = 160 g/mol), the molecular weight of MINP(**2**) translates to 50 [= 42100 / (0.6×535 + 0.4×558 + 0.6×264 + 130 + 0.02×160)] of such units.

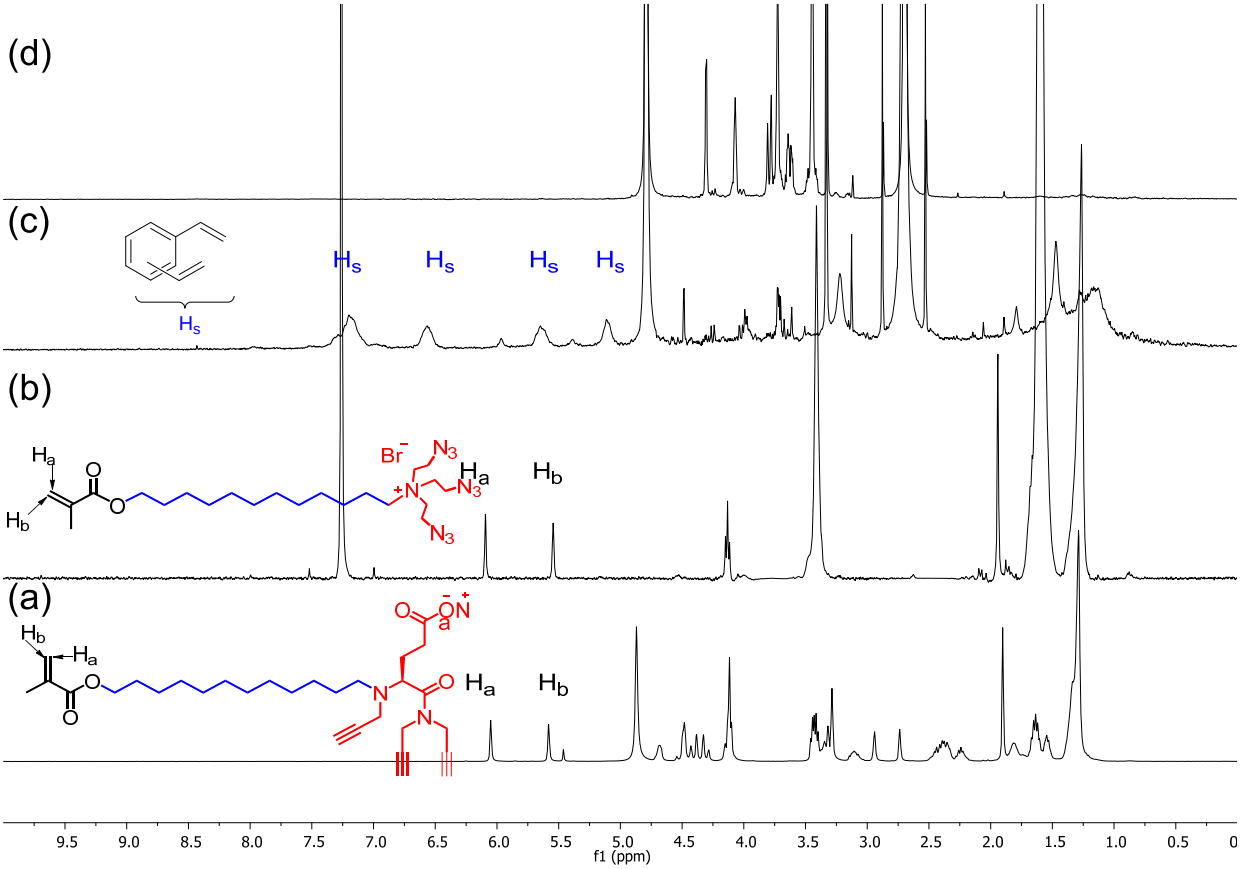

Figure S9. ^{1}H NMR spectra of (a) Compound **6** in CD_3OD, (b) Compound **7** in $CDCl_3$, (c) alkynyl-SCM in D_2O, and (d) MINP(**2**) in D_2O at 298 K.

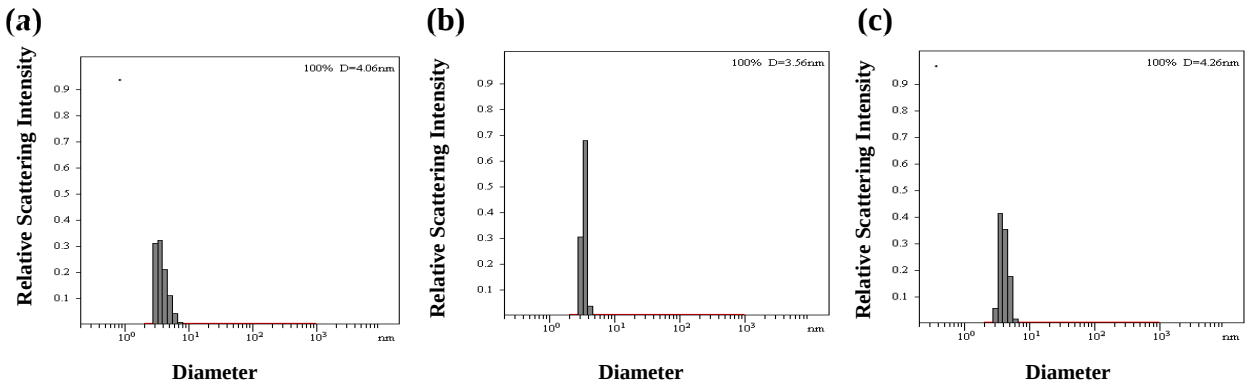

Figure S10. Distribution of the hydrodynamic diameters of the nanoparticles in water as determined by DLS for the synthesis of MINP(psychosine) (a) alkynyl-SCM, (b) core-cross-linked-SCM, and (c) surface-functionalized MINP(**3**) after purification.

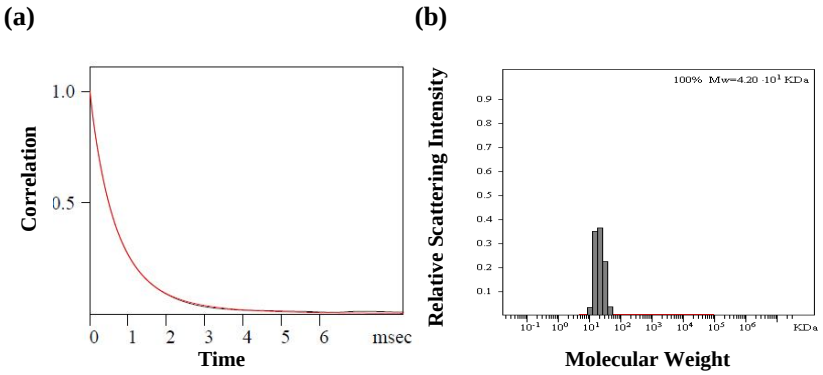

Figure S11. The correlation curve and the distribution of the molecular weight for MINP(**3**) from the DLS. The PRECISION DECONVOLVE program assumes the intensity of scattering is proportional to the mass of the particle squared. If each unit of building block for the MINP(**1**) is assumed to contain 0.6 molecules of Compound **6** (MW = 535 g/mol), 0.4 molecules of compound **7** (MW = 558 g/mol), 0.6 molecules of compound **9** (MW = 264 g/mol), one molecule of DVB (MW = 130 g/mol), and 0.02 molecules of 6-vinylbenzoxaborole (MW = 160 g/mol), the molecular weight of MINP(**3**) translates to 50 [= 42000 / (0.6×535 + 0.4×558 + 0.6×264 + 130 + 0.02×160)] of such units.

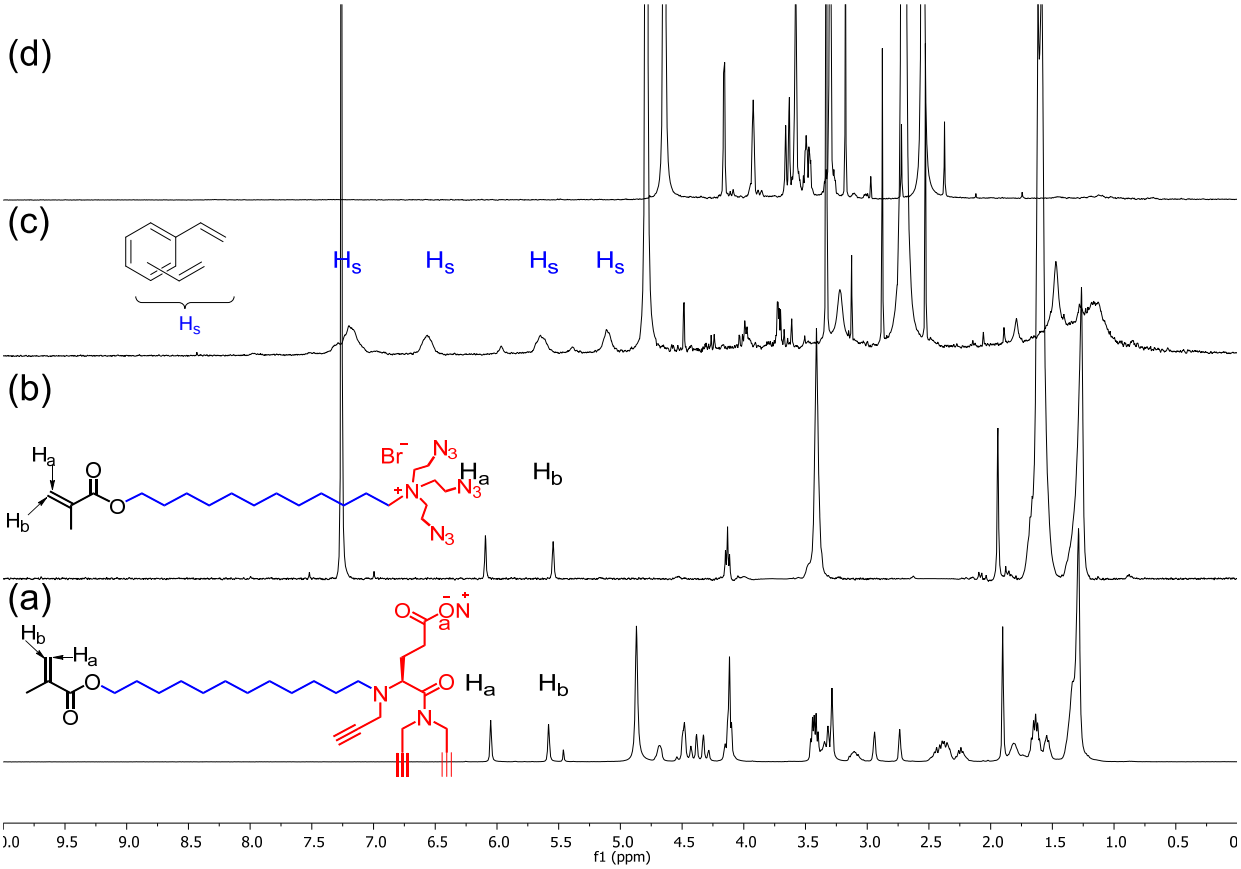

Figure S12. ^{1}H NMR spectra of (a) Compound **6** in CD_3OD, (b) Compound **7** in $CDCl_3$, (c) alkynyl-SCM in D_2O, and (d) MINP(**4**) in D_2O at 298 K.

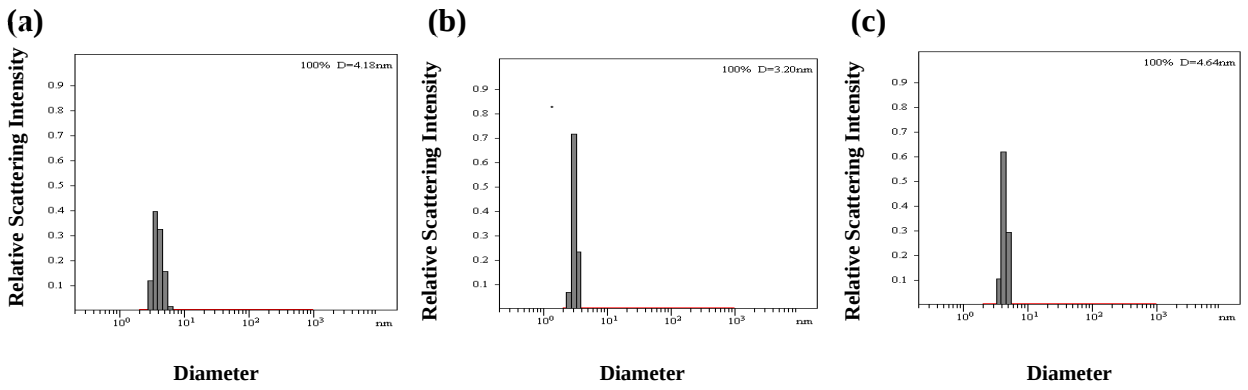

Figure S13. Distribution of the hydrodynamic diameters of the nanoparticles in water as determined by DLS for the synthesis of MINP(glucosylceramide) (a) alkynyl-SCM, (b) core-cross-linked-SCM, and (c) surface-functionalized MINP(**4**) after purification.

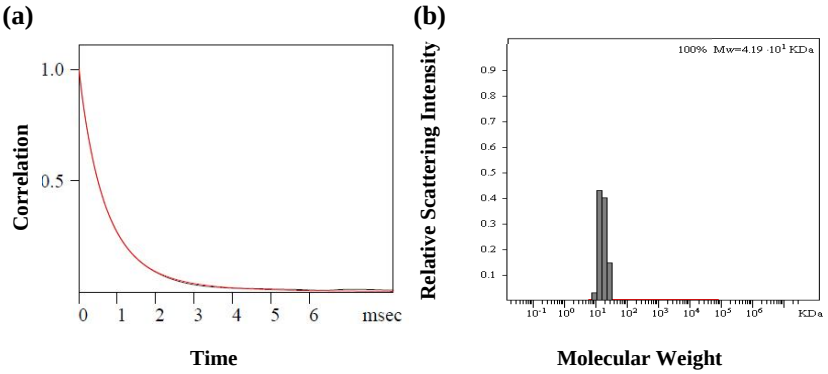

Figure S14. The correlation curve and the distribution of the molecular weight for MINP(**4**) from the DLS. The PRECISION DECONVOLVE program assumes the intensity of scattering is proportional to the mass of the particle squared. If each unit of building block for the MINP(**1**) is assumed to contain 0.6 molecules of Compound **6** (MW = 535 g/mol), 0.4 molecules of compound **7** (MW = 558 g/mol), 0.6 molecules of compound **9** (MW = 264 g/mol), one molecule of DVB (MW = 130 g/mol), and 0.02 molecules of 6-vinylbenzoxaborole (MW = 160 g/mol), the molecular weight of MINP(**4**) translates to 50 [= 41900 / (0.6×535 + 0.4×558 + 0.6×264 + 130 + 0.02×160)] of such units.

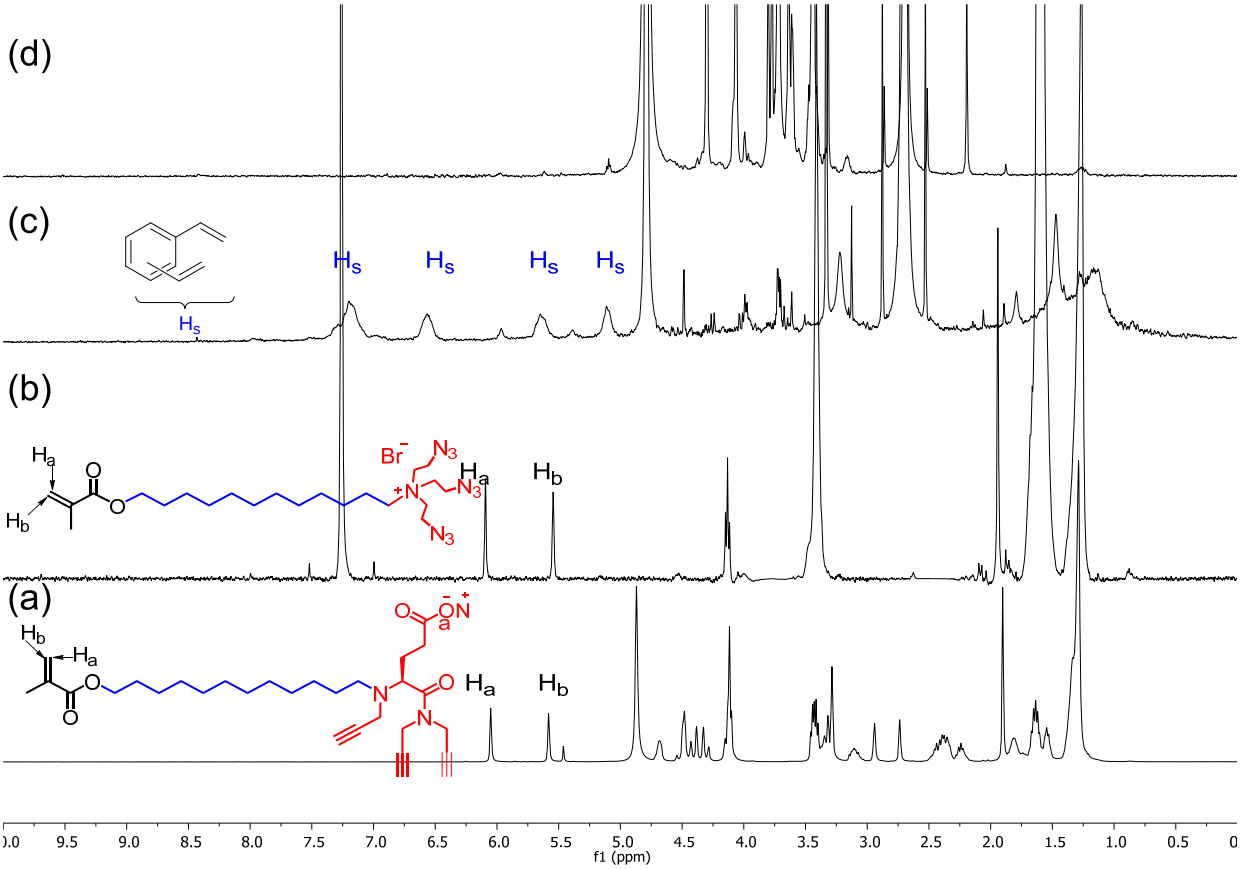

Figure S15. ^{1}H NMR spectra of (a) Compound **6** in CD_3OD, (b) Compound **7** in $CDCl_3$, (c) alkynyl-SCM in D_2O, and (d) MINP(lactosylceramide) in D_2O at 298 K.

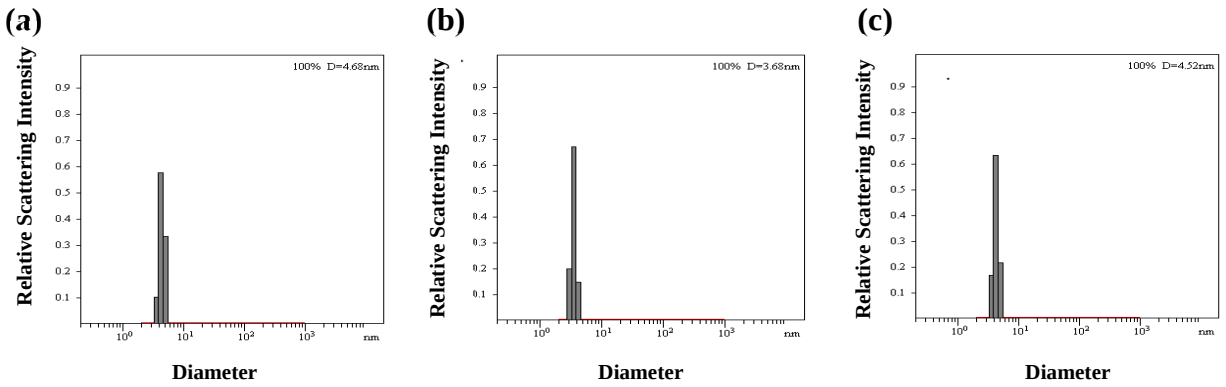

Figure S16. Distribution of the hydrodynamic diameters of the nanoparticles in water as determined by DLS for the synthesis of MINP(**5**) (a) alkynyl-SCM, (b) core-cross-linked-SCM, and (c) surface-functionalized MINP(**5**) after purification.

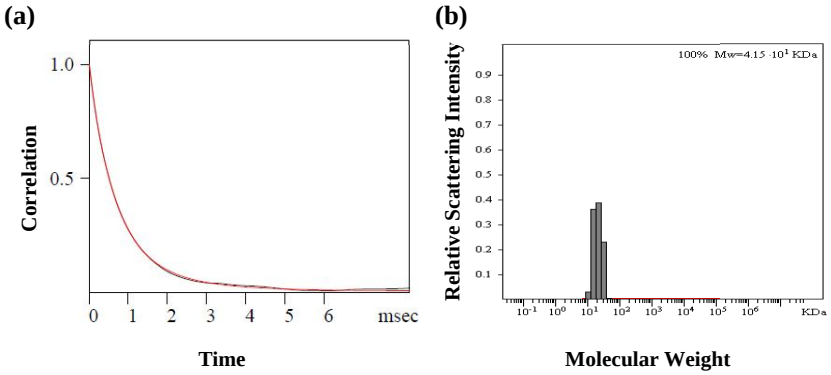

Figure S17. The correlation curve and the distribution of the molecular weight for MINP(**5**) from the DLS. The PRECISION DECONVOLVE program assumes the intensity of scattering is proportional to the mass of the particle squared. If each unit of building block for the MINP(**1**) is assumed to contain 0.6 molecules of Compound **6** (MW = 535 g/mol), 0.4 molecules of compound **7** (MW = 558 g/mol), 0.6 molecules of compound **9** (MW = 264 g/mol), one molecule of DVB (MW = 130 g/mol), and 0.02 molecules of 6-vinylbenzoxaborole (MW = 160 g/mol), the molecular weight of MINP(**5**) translates to 50 [= 41500 / (0.6×535 + 0.4×558 + 0.6×264 + 130 + 0.02×160)] of such units.

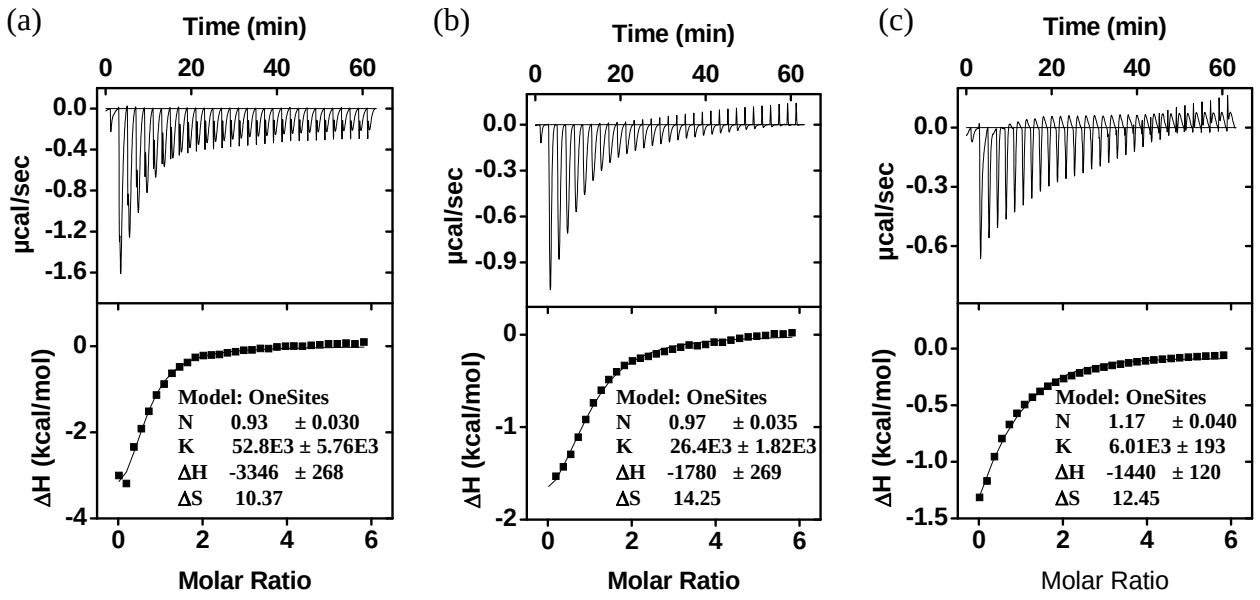

Figure S18. ITC titration curves obtained at 298 K for the titration of MINP(**1**) with (a) kerasin **1**, (b) phrenosin **2**, and (c) psychosine **3** in 10 mM HEPES buffer (pH 7.4, template/FM **8** = 1:1) containing 0.1% Tween-20 detergent. The data correspond to entries 1–3, respectively, in Table 1. The top panel shows the raw calorimetric data. The area under each peak represents the amount of heat generated at each ejection and is plotted against the molar ratio of MINP to the substrate. The solid line is the best fit of the experimental data to the sequential binding of N equal and independent binding sites on the MINP. The heat of dilution for the substrate, obtained by adding the substrate to the buffer, was subtracted from the heat released during the binding. Binding parameters were auto-generated after curve fitting using Microcal Origin 7.

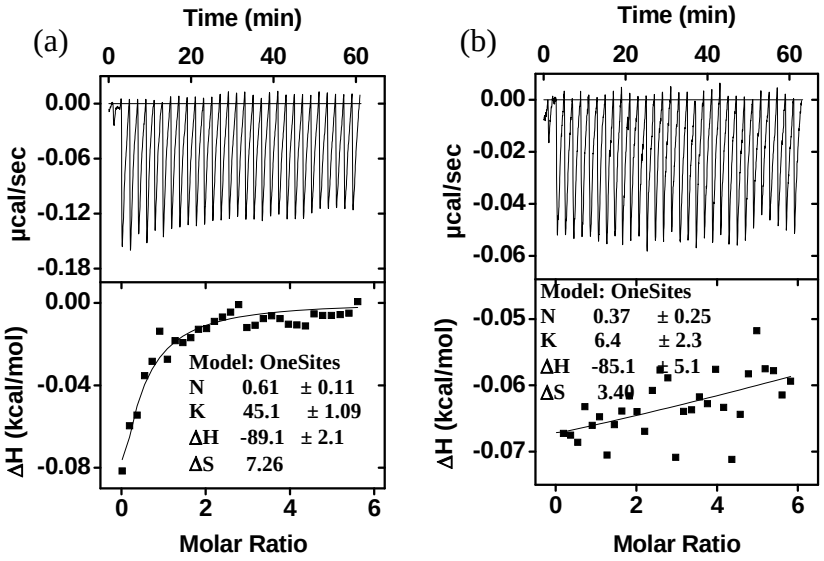

Figure S19. ITC titration curves obtained at 298 K for the titration of MINP(**1**) with (a) glucosylceramide **4** and (b) lactosylceramide **5** in 10 mM HEPES buffer (pH 7.4, template/FM **8** = 1:1) containing 0.1% Tween-20 detergent. The data correspond to entries 4–5, respectively, in Table 1. The top panel shows the raw calorimetric data. The area under each peak represents the amount of heat generated at each ejection and is plotted against the molar ratio of MINP to the substrate. The solid line is the best fit of the experimental data to the sequential binding of N equal and independent binding sites on the MINP. The heat of dilution for the substrate, obtained by adding the substrate to the buffer, was subtracted from the heat released during the binding. Binding parameters were auto-generated after curve fitting using Microcal Origin 7.

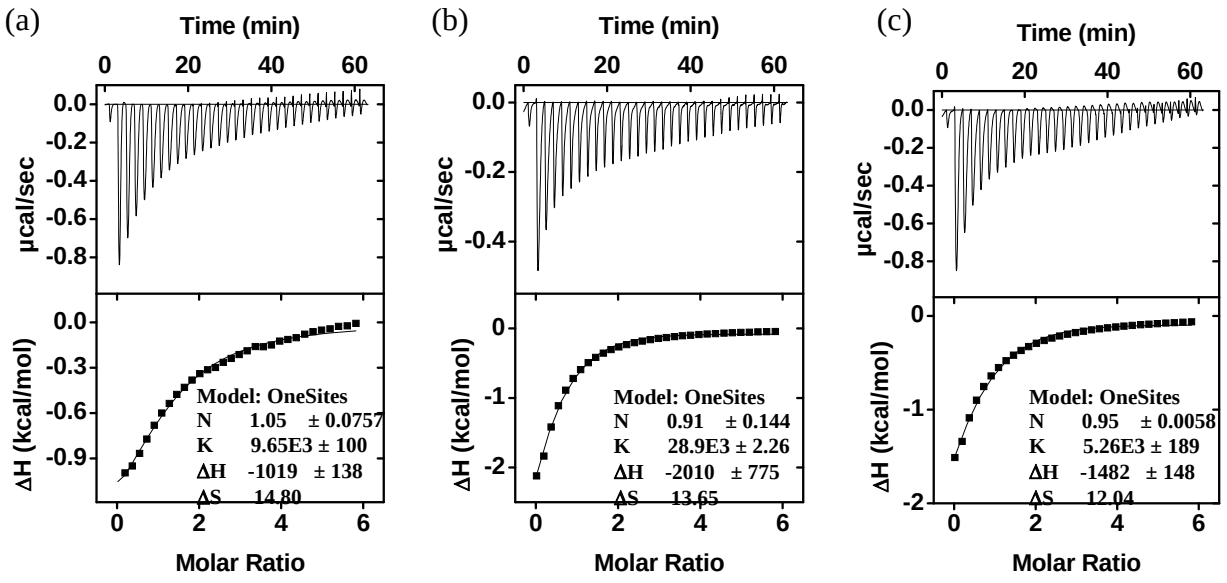

Figure S20. ITC titration curves obtained at 298 K for the titration of MINP(**2**) with (a) kerasin **1**, (b) phrenosin **2**, and (c) psychosine **3** in 10 mM HEPES buffer (pH 7.4, template/FM **8** = 1:1) containing 0.1% Tween-20 detergent. The data correspond to entries 6–8, respectively, in Table 1. The top panel shows the raw calorimetric data. The area under each peak represents the amount of heat generated at each ejection and is plotted against the molar ratio of MINP to the substrate. The solid line is the best fit of the experimental data to the sequential binding of N equal and independent binding sites on the MINP. The heat of dilution for the substrate, obtained by adding the substrate to the buffer, was subtracted from the heat released during the binding. Binding parameters were auto-generated after curve fitting using Microcal Origin 7.

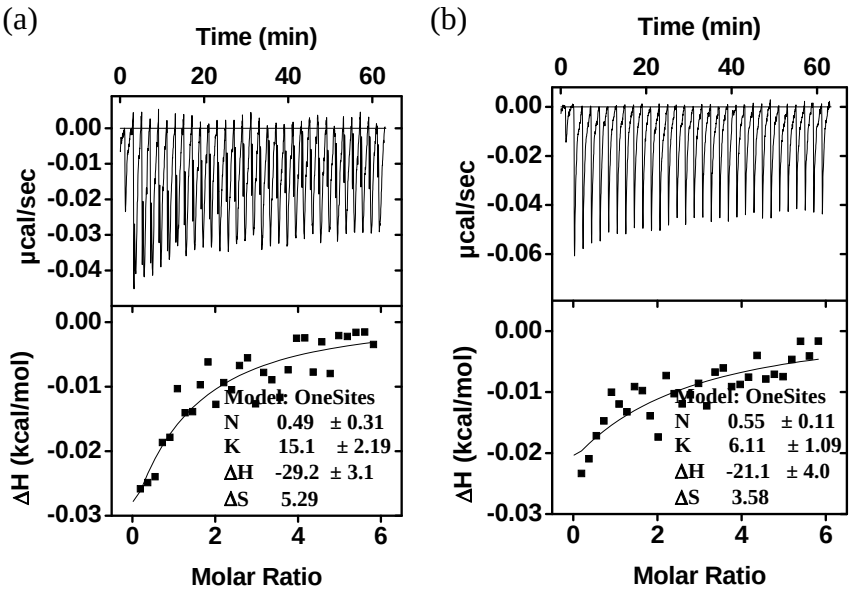

Figure S21. ITC titration curves obtained at 298 K for the titration of MINP(**2**) with (a) glucosylceramide **4** and (b) lactosylceramide **5** in 10 mM HEPES buffer (pH 7.4, template/FM **8** = 1:1) containing 0.1% Tween-20 detergent. The data correspond to entries 9–10, respectively, in Table 1. The top panel shows the raw calorimetric data. The area under each peak represents the amount of heat generated at each ejection and is plotted against the molar ratio of MINP to the substrate. The solid line is the best fit of the experimental data to the sequential binding of N equal and independent binding sites on the MINP. The heat of dilution for the substrate, obtained by adding the substrate to the buffer, was subtracted from the heat released during the binding. Binding parameters were auto-generated after curve fitting using Microcal Origin 7.

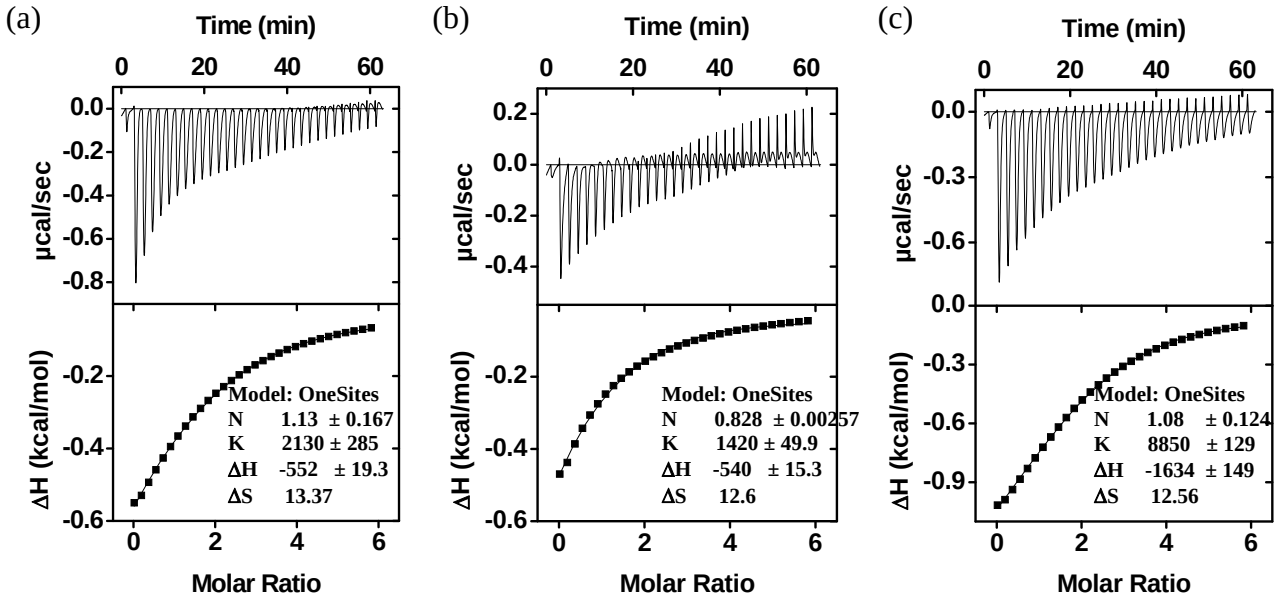

Figure S22. ITC titration curves obtained at 298 K for the titration of MINP(**3**) with (a) kerasin **1**, (b) phrenosin **2**, and (c) psychosine **3** in 10 mM HEPES buffer (pH 7.4, template/FM **8** = 1:1) containing 0.1% Tween-20 detergent. The data correspond to entries 11–13, respectively, in Table 1. The top panel shows the raw calorimetric data. The area under each peak represents the amount of heat generated at each ejection and is plotted against the molar ratio of MINP to the substrate. The solid line is the best fit of the experimental data to the sequential binding of N equal and independent binding sites on the MINP. The heat of dilution for the substrate, obtained by adding the substrate to the buffer, was subtracted from the heat released during the binding. Binding parameters were auto-generated after curve fitting using Microcal Origin 7.

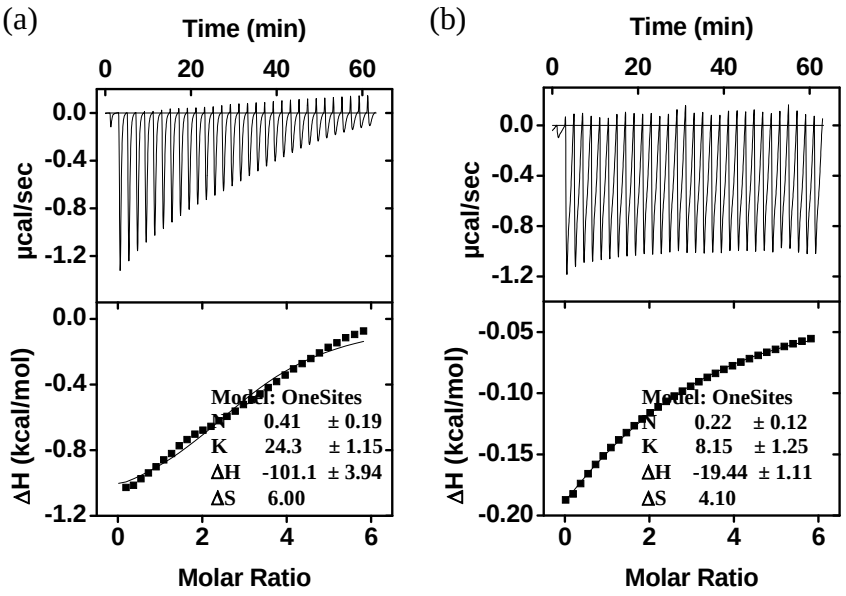

Figure S23. ITC titration curves obtained at 298 K for the titration of MINP(**3**) with (a) glucosylceramide **4** and (b) lactosylceramide **5** in 10 mM HEPES buffer (pH 7.4, template/FM **8** = 1:1) containing 0.1% Tween-20 detergent. The data correspond to entries 14–15, respectively, in Table 1. The top panel shows the raw calorimetric data. The area under each peak represents the amount of heat generated at each ejection and is plotted against the molar ratio of MINP to the substrate. The solid line is the best fit of the experimental data to the sequential binding of N equal and independent binding sites on the MINP. The heat of dilution for the substrate, obtained by adding the substrate to the buffer, was subtracted from the heat released during the binding. Binding parameters were auto-generated after curve fitting using Microcal Origin 7.

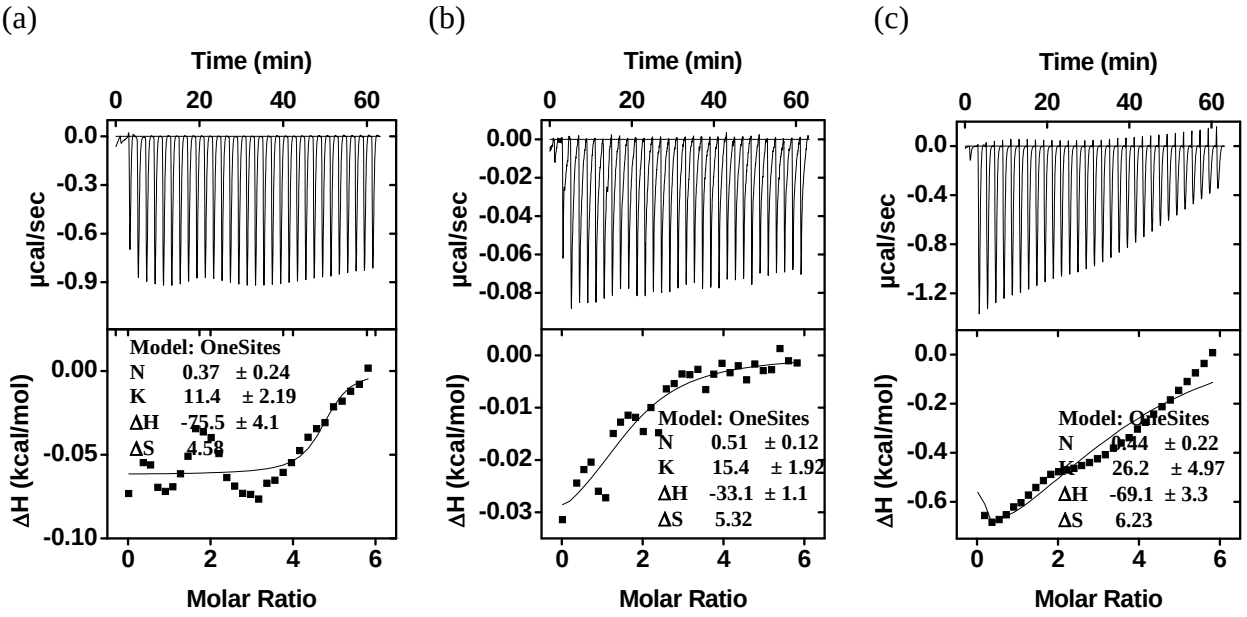

Figure S24. ITC titration curves obtained at 298 K for the titration of MINP(**4**) with (a) kerasin **1**, (b) phrenosin **2**, and (c) psychosine **3** in 10 mM HEPES buffer (pH 7.4, template/FM **8** = 1:1) containing 0.1% Tween-20 detergent. The data correspond to entries 16–18, respectively, in Table 1. The top panel shows the raw calorimetric data. The area under each peak represents the amount of heat generated at each ejection and is plotted against the molar ratio of MINP to the substrate. The solid line is the best fit of the experimental data to the sequential binding of N equal and independent binding sites on the MINP. The heat of dilution for the substrate, obtained by adding the substrate to the buffer, was subtracted from the heat released during the binding. Binding parameters were auto-generated after curve fitting using Microcal Origin 7.

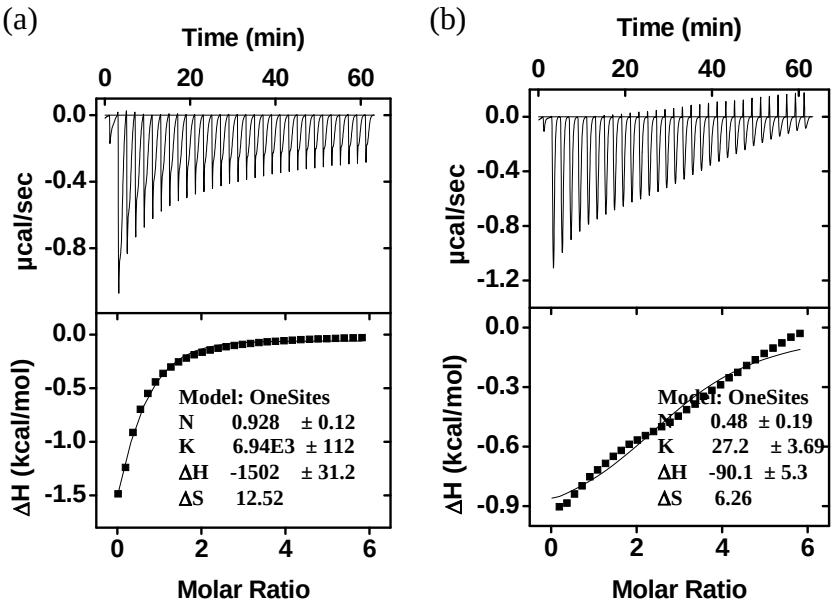

Figure S25. ITC titration curves obtained at 298 K for the titration of MINP(**4**) with (a) glucosylceramide **4** and (b) lactosylceramide **5** in 10 mM HEPES buffer (pH 7.4, template/FM **8** = 1:1) containing 0.1% Tween-20 detergent. The data correspond to entries 19–20, respectively, in Table 1. The top panel shows the raw calorimetric data. The area under each peak represents the amount of heat generated at each ejection and is plotted against the molar ratio of MINP to the substrate. The solid line is the best fit of the experimental data to the sequential binding of N equal and independent binding sites on the MINP. The heat of dilution for the substrate, obtained by adding the substrate to the buffer, was subtracted from the heat released during the binding. Binding parameters were auto-generated after curve fitting using Microcal Origin 7.

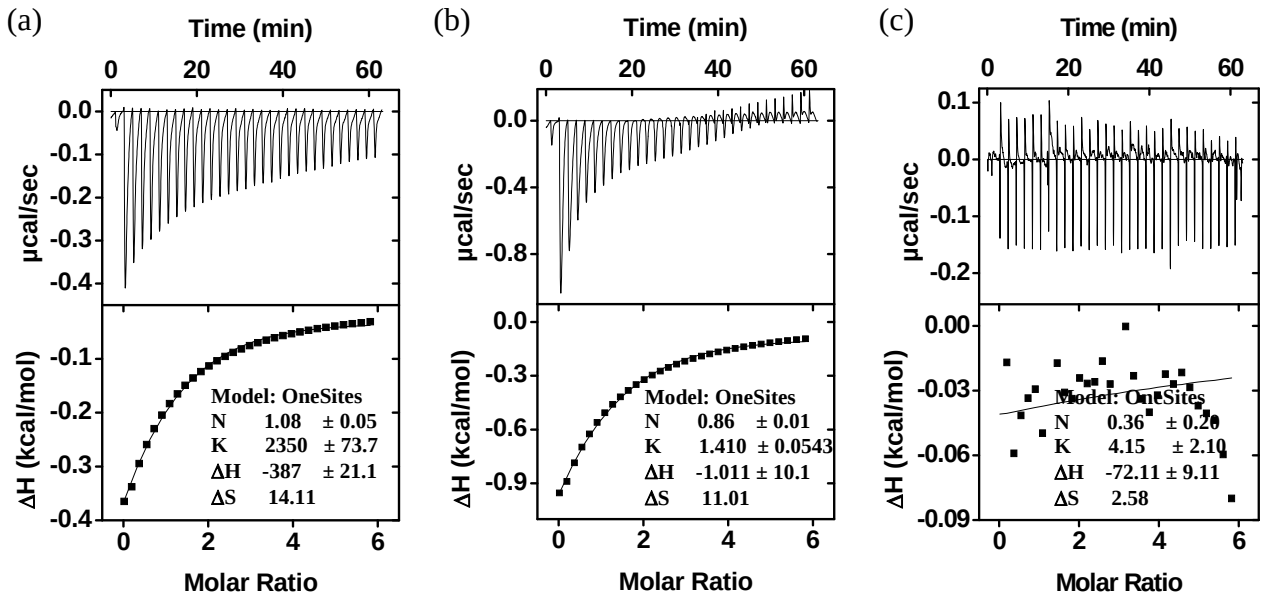

Figure S26. ITC titration curves obtained at 298 K for the titration of MINP(**5**) with (a) kerasin **1**, (b) phrenosin **2**, and (c) psychosine **3** in 10 mM HEPES buffer (pH 7.4, template/FM **8** = 1:1) containing 0.1% Tween-20 detergent. The data correspond to entries 21–23, respectively, in Table 1. The top panel shows the raw calorimetric data. The area under each peak represents the amount of heat generated at each ejection and is plotted against the molar ratio of MINP to the substrate. The solid line is the best fit of the experimental data to the sequential binding of N equal and independent binding sites on the MINP. The heat of dilution for the substrate, obtained by adding the substrate to the buffer, was subtracted from the heat released during the binding. Binding parameters were auto-generated after curve fitting using Microcal Origin 7.

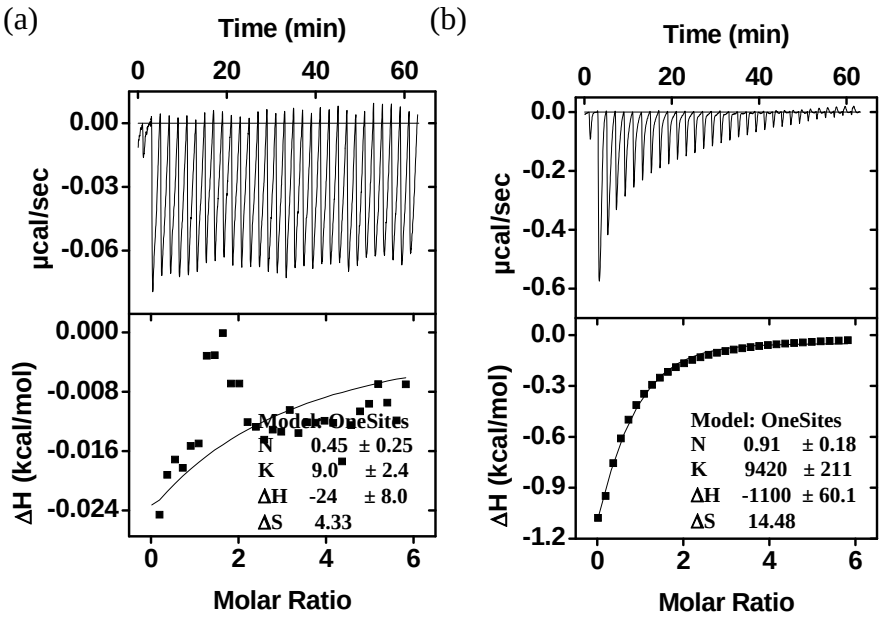

Figure S27. ITC titration curves obtained at 298 K for the titration of MINP(**5**) with (a) glucosylceramide **4** and (b) lactosylceramide **5** in 10 mM HEPES buffer (pH 7.4, template/FM **8** = 1:1) containing 0.1% Tween-20 detergent. The data correspond to entries 24–25, respectively, in Table 1. The top panel shows the raw calorimetric data. The area under each peak represents the amount of heat generated at each ejection and is plotted against the molar ratio of MINP to the substrate. The solid line is the best fit of the experimental data to the sequential binding of N equal and independent binding sites on the MINP. The heat of dilution for the substrate, obtained by adding the substrate to the buffer, was subtracted from the heat released during the binding. Binding parameters were auto-generated after curve fitting using Microcal Origin 7.

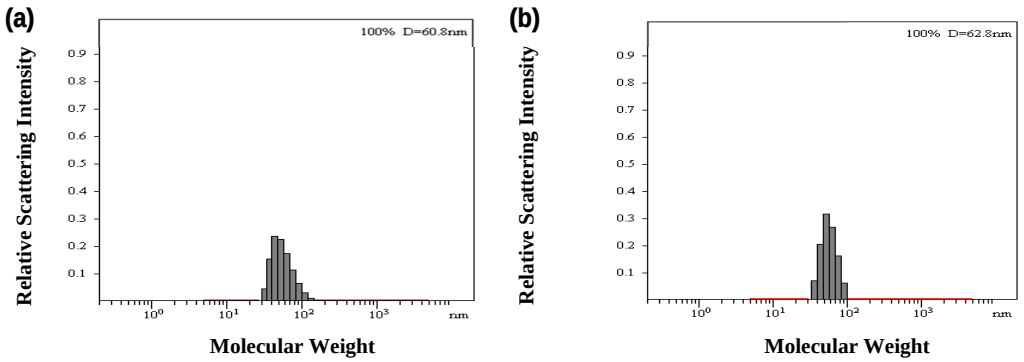

Figure S28. Distribution of the hydrodynamic diameters of the liposomes prepared in HEPES buffer (1.0 mL, pH = 7.4) with 1% POPC/POPG 1/0 by 30 nm filter at (a) 0 h and (b) 2 h as determined by DLS. Average size obtained from DLS: 61 ± 3 nm.

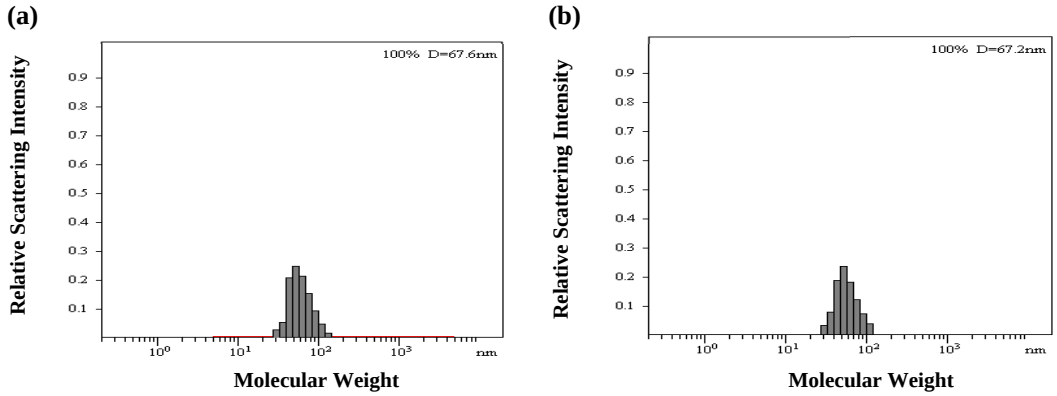

Figure S29. Distribution of the hydrodynamic diameters of the liposomes prepared in HEPES buffer (1.0 mL, pH = 7.4) with 1% POPC/POPG 20/1 by 30 nm filter at (a) 0 h and (b) 2 h as determined by DLS. Average size obtained from DLS: 67 ± 2 nm.

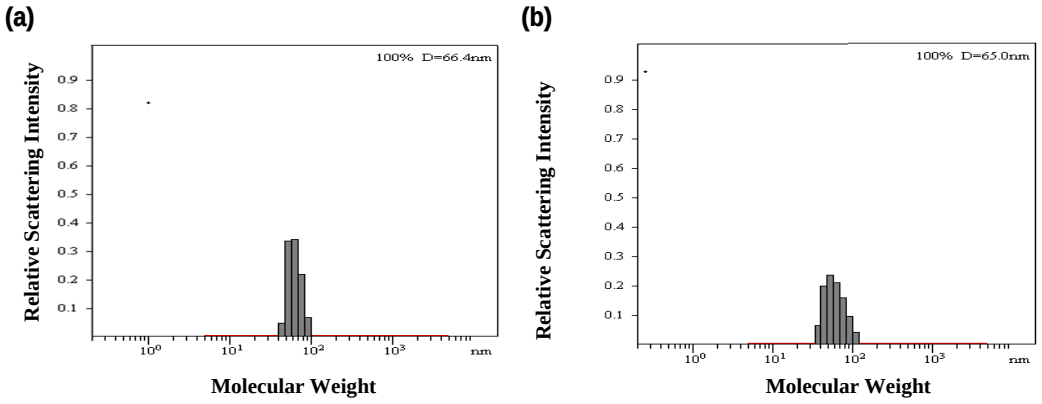

Figure S30. Distribution of the hydrodynamic diameters of the liposomes prepared in HEPES buffer (1.0 mL, pH = 7.4) with 1% POPC/POPG 5/1 by 30 nm filter at (a) 0 h and (b) 2 h as determined by DLS. Average size obtained from DLS: 65 ± 2 nm.

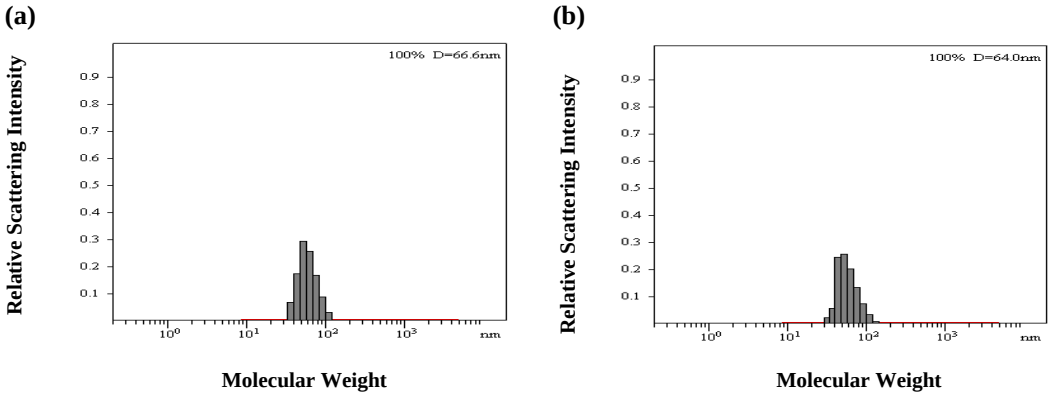

Figure S31. Distribution of the hydrodynamic diameters of the liposomes prepared in HEPES buffer (1.0 mL, pH = 7.4) with 1% POPC/POPG 0/1 by 30 nm filter at (a) 0 h and (b) 2 h as determined by DLS. Average size obtained from DLS: 65 ± 3 nm.

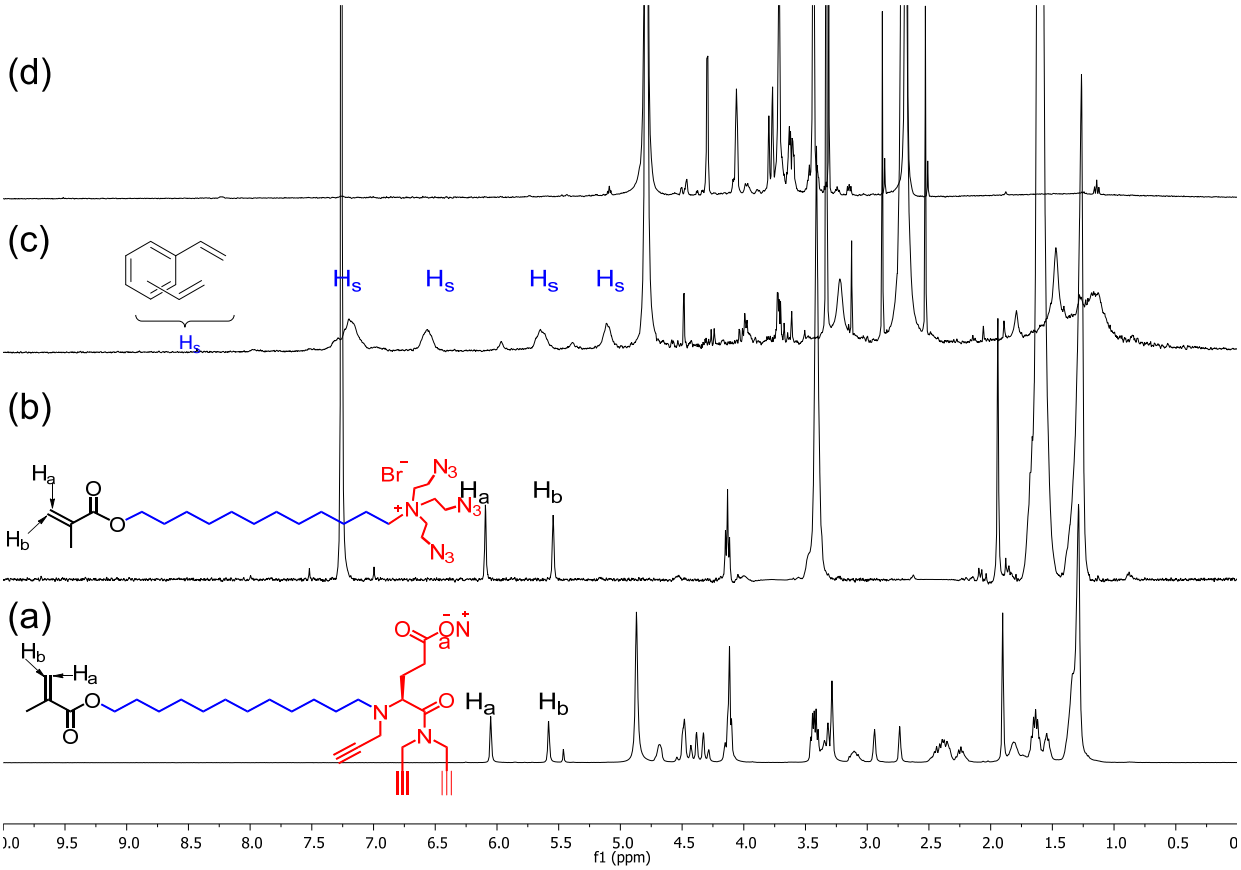

Figure S32. ^{1}H NMR spectra of (a) Compound **6** in CD_3OD, (b) Compound **7** in $CDCl_3$, (c) alkynyl-SCM in D_2O, and (d) MINP(**10**) in D_2O at 298 K.

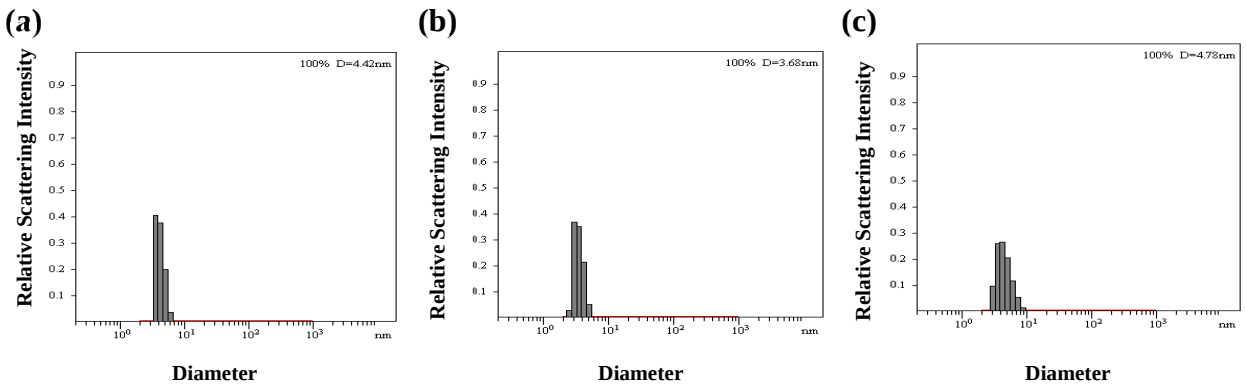

Figure S33. Distribution of the hydrodynamic diameters of the nanoparticles in water as determined by DLS for the synthesis of MINP(**10**) (a) alkynyl-SCM, (b) core-cross-linked-SCM, and (c) surface-functionalized MINP(**10**) after purification.

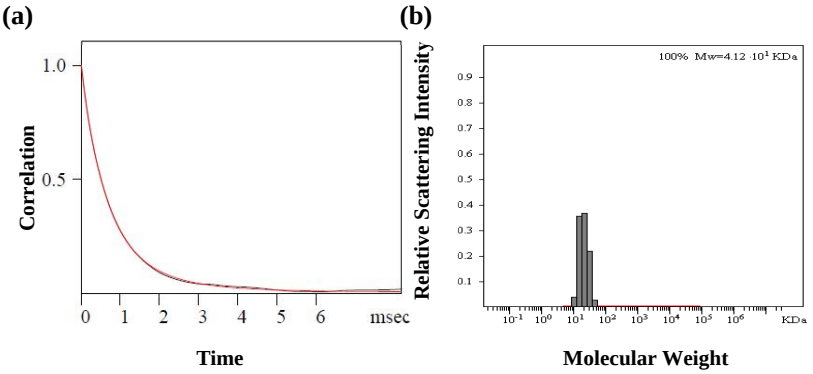

Figure S34. The correlation curve and the distribution of the molecular weight for MINP(**10**) from the DLS. The PRECISION DECONVOLVE program assumes the intensity of scattering is proportional to the mass of the particle squared. If each unit of building block for the MINP(**1**) is assumed to contain 0.6 molecules of Compound **6** (MW = 535 g/mol), 0.4 molecules of compound **7** (MW = 558 g/mol), 0.6 molecules of compound **9** (MW = 264 g/mol), one molecule of DVB (MW = 130 g/mol), and 0.02 molecules of 6-vinylbenzoxaborole (MW = 160 g/mol), the molecular weight of MINP(**10**) translates to 49 [= 41200 / (0.6×535 + 0.4×558 + 0.6×264 + 130 + 0.02×160)] of such units.

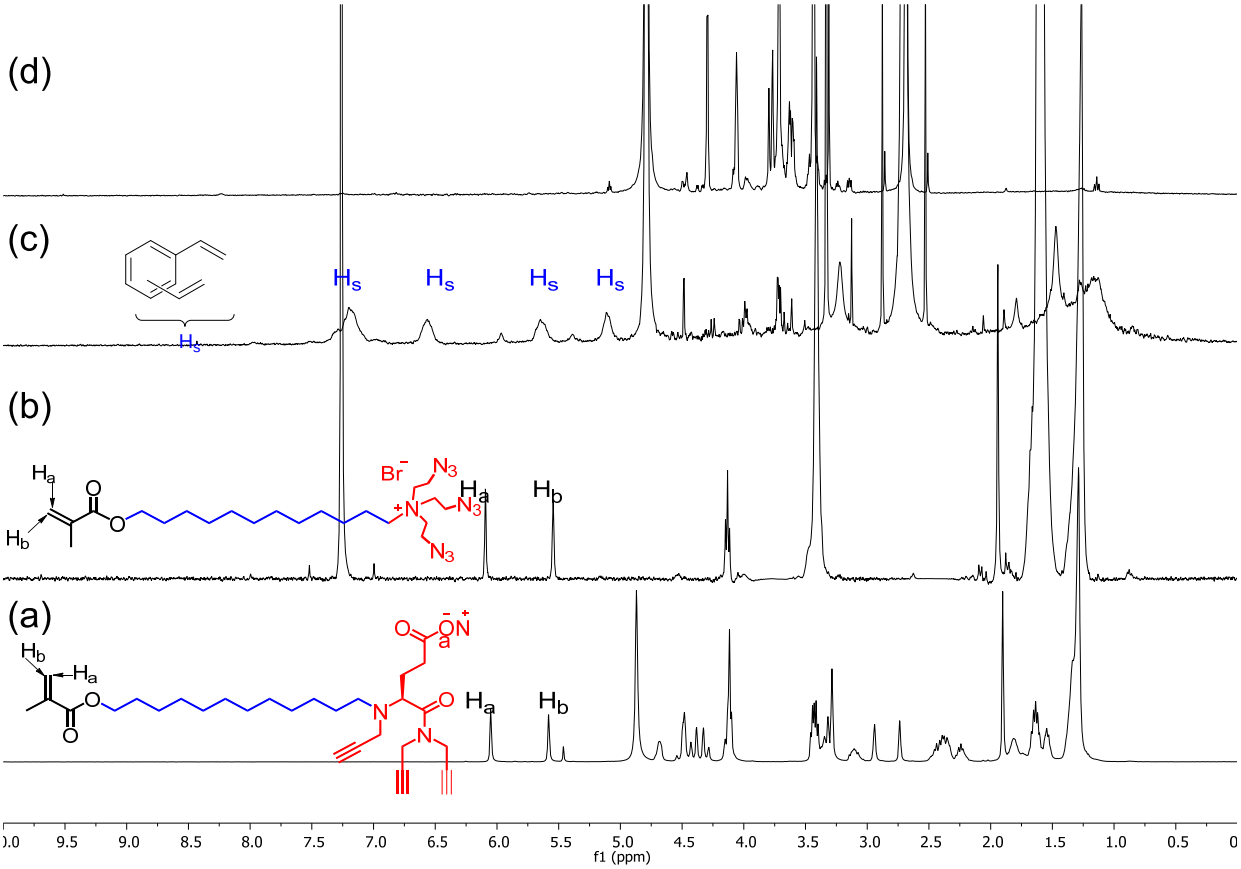

Figure S35. ^{1}H NMR spectra of (a) Compound **6** in CD_3OD, (b) Compound **7** in $CDCl_3$, (c) alkynyl-SCM in D_2O, and (d) MINP(**11**) in D_2O at 298 K.

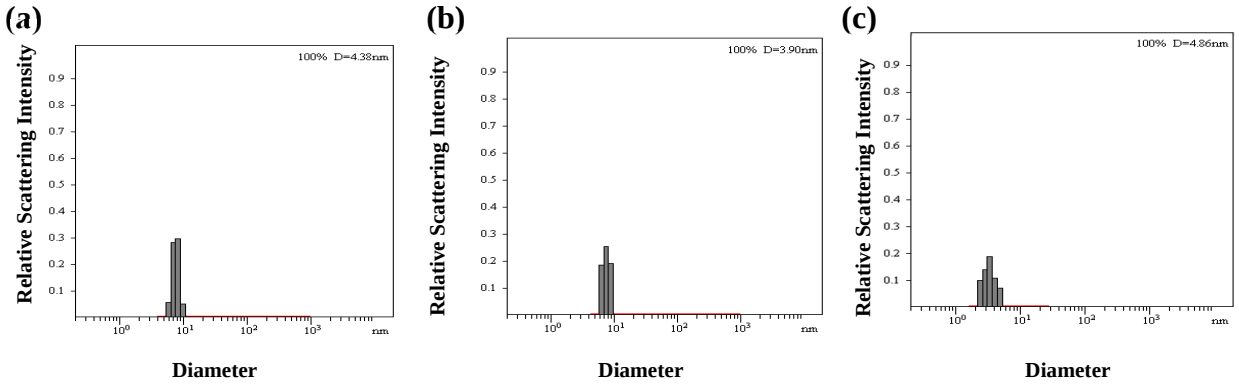

Figure S36. Distribution of the hydrodynamic diameters of the nanoparticles in water as determined by DLS for the synthesis of MINP(**11**) (a) alkynyl-SCM, (b) core-cross-linked-SCM, and (c) surface-functionalized MINP(**11**) after purification.

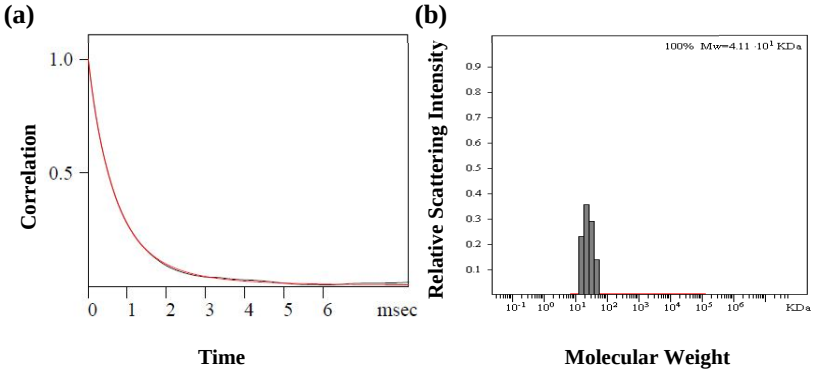

Figure S37. The correlation curve and the distribution of the molecular weight for MINP(**11**) from the DLS. The PRECISION DECONVOLVE program assumes the intensity of scattering is proportional to the mass of the particle squared. If each unit of building block for the MINP(**1**) is assumed to contain 0.6 molecules of Compound **6** (MW = 535 g/mol), 0.4 molecules of compound **7** (MW = 558 g/mol), 0.6 molecules of compound **9** (MW = 264 g/mol), one molecule of DVB (MW = 130 g/mol), and 0.02 molecules of 6-vinylbenzoxaborole (MW = 160 g/mol), the molecular weight of MINP(**11**) translates to 49 [= 41100 / (0.6×535 + 0.4×558 + 0.6×264 + 130 + 0.02×160)] of such units.

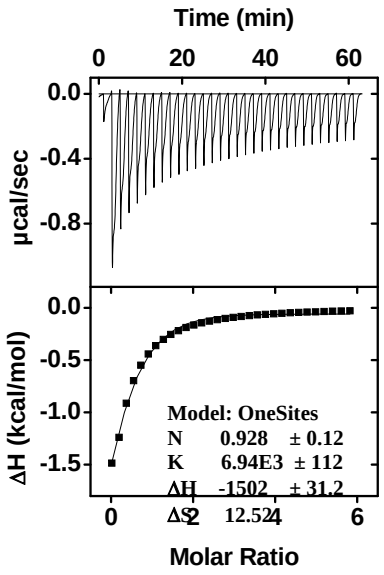

Figure S38. ITC titration curves obtained at 298 K for the titration of MINP(**4**) with glucosylceramide **4** in 10 mM HEPES buffer (pH 7.4, template/FM **8** = 1:1) containing 0.1% Tween-20 detergent. The data correspond to entry 1 in Table 2. The top panel shows the raw calorimetric data. The area under each peak represents the amount of heat generated at each ejection and is plotted against the molar ratio of MINP to the substrate. The solid line is the best fit of the experimental data to the sequential binding of N equal and independent binding sites on the MINP. The heat of dilution for the substrate, obtained by adding the substrate to the buffer, was subtracted from the heat released during the binding. Binding parameters were auto-generated after curve fitting using Microcal Origin 7.

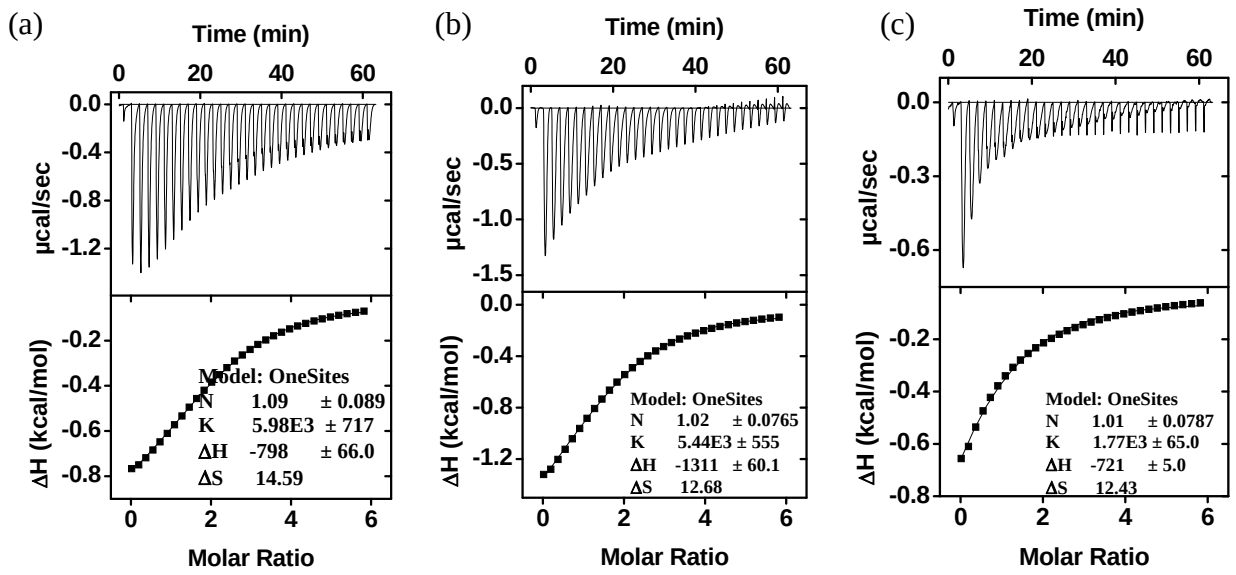

Figure S39. ITC titration curves obtained at 298 K for the titration of MINP(**4**) with glucosylceramide **4** in 10 mM HEPES buffer (pH 7.4, template/FM **8** = 1:1) containing 1% (a) POPC, (b) POPC/POPG 20:1, and (c) POPC/POPG 5:1. The data correspond to entries 2–4, respectively, in Table 2. The top panel shows the raw calorimetric data. The area under each peak represents the amount of heat generated at each ejection and is plotted against the molar ratio of MINP to the substrate. The solid line is the best fit of the experimental data to the sequential binding of N equal and independent binding sites on the MINP. The heat of dilution for the substrate, obtained by adding the substrate to the buffer, was subtracted from the heat released during the binding. Binding parameters were auto-generated after curve fitting using Microcal Origin 7.

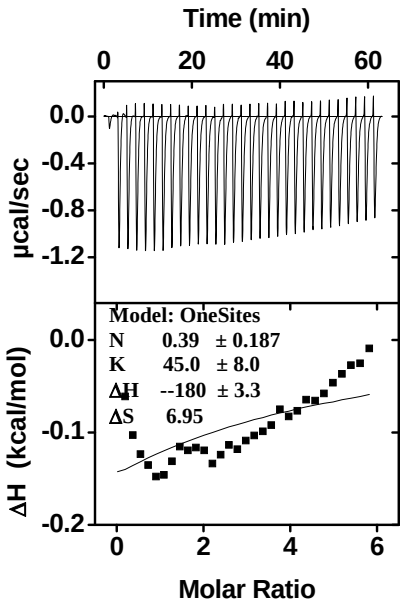

Figure S40. ITC titration curves obtained at 298 K for the titration of MINP(**4**) with glucosylceramide **4** in10 mM HEPES buffer (pH 7.4, template/FM **8** = 1:1) containing 1% POPG. The data correspond to entry 5 in Table 2. The top panel shows the raw calorimetric data. The area under each peak represents the amount of heat generated at each ejection and is plotted against the molar ratio of MINP to the substrate. The solid line is the best fit of the experimental data to the sequential binding of N equal and independent binding sites on the MINP. The heat of dilution for the substrate, obtained by adding the substrate to the buffer, was subtracted from the heat released during the binding. Binding parameters were auto-generated after curve fitting using Microcal Origin 7.

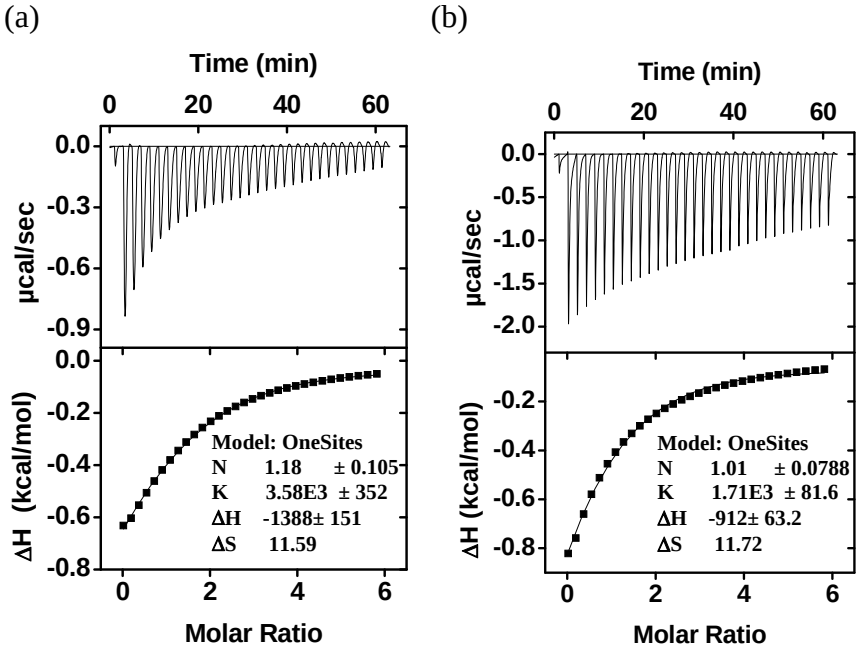

Figure S41. ITC titration curves obtained at 298 K for the titration of MINP(**10**) with (a) octyl β-D-glucopyranoside **10** and (b) glucosylceramide **4** in 10 mM HEPES buffer (pH 7.4, template/FM **8** = 1:1) containing 1% POPC. The data correspond to entries 6–7, respectively, in Table 2. The top panel shows the raw calorimetric data. The area under each peak represents the amount of heat generated at each ejection and is plotted against the molar ratio of MINP to the substrate. The solid line is the best fit of the experimental data to the sequential binding of N equal and independent binding sites on the MINP. The heat of dilution for the substrate, obtained by adding the substrate to the buffer, was subtracted from the heat released during the binding. Binding parameters were auto-generated after curve fitting using Microcal Origin 7.

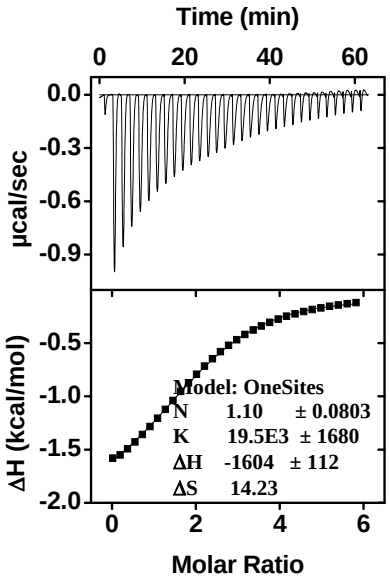

Figure S42. ITC titration curves obtained at 298 K for the titration of MINP(**10**) with (a) octyl β-D-glucopyranoside **10** in 10 mM HEPES buffer (pH 7.4, template/FM **8** = 1:1). The data correspond to entry 8 in Table 2. The top panel shows the raw calorimetric data. The area under each peak represents the amount of heat generated at each ejection and is plotted against the molar ratio of MINP to the substrate. The solid line is the best fit of the experimental data to the sequential binding of N equal and independent binding sites on the MINP. The heat of dilution for the substrate, obtained by adding the substrate to the buffer, was subtracted from the heat released during the binding. Binding parameters were auto-generated after curve fitting using Microcal Origin 7.

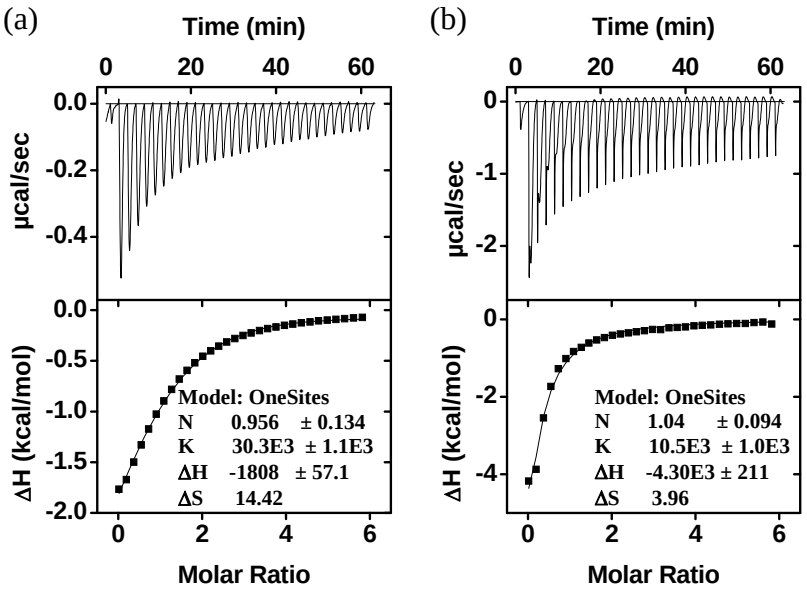

Figure S43. ITC titration curves obtained at 298 K for the titration of MINP(**11**) with (a) 4-nitrophenyl-α-D-glucopyranoside **11** and (b) octyl β-D-glucopyranoside **10** in 10 mM HEPES buffer (pH 7.4, template/FM **4** = 1:1). The data correspond to entries 9–10, respectively, in Table 2. The top panel shows the raw calorimetric data. The area under each peak represents the amount of heat generated at each ejection and is plotted against the molar ratio of MINP to the substrate. The solid line is the best fit of the experimental data to the sequential binding of N equal and independent binding sites on the MINP. The heat of dilution for the substrate, obtained by adding the substrate to the buffer, was subtracted from the heat released during the binding. Binding parameters were auto-generated after curve fitting using Microcal Origin 7.

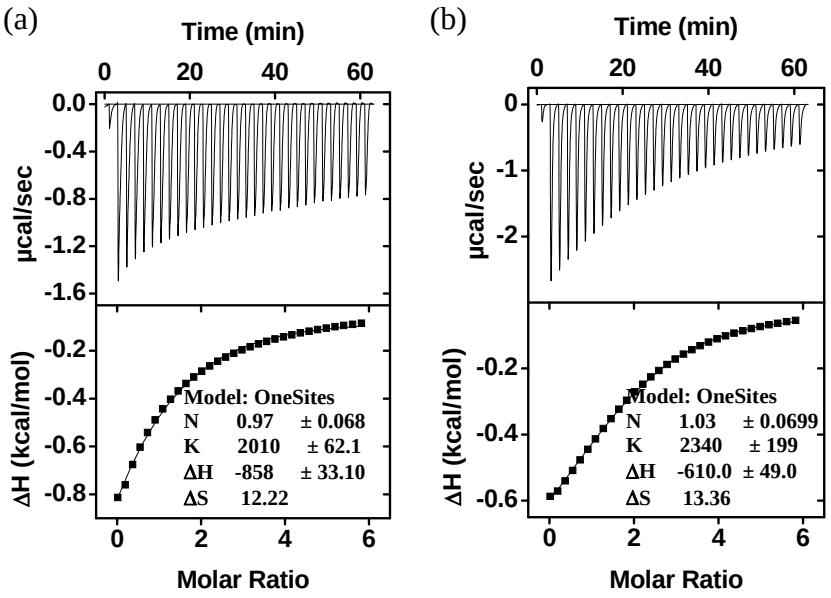

Figure S44. ITC titration curves obtained at 298 K for the titration of MINP(**11**) with (a) octyl β-D-glucopyranoside **10** and (b) glucosylceramide **4** in 10 mM HEPES buffer (pH 7.4, template/FM **8** = 1:1) containing 1% POPC. The data correspond to entries 11–12, respectively, in Table 2. The top panel shows the raw calorimetric data. The area under each peak represents the amount of heat generated at each ejection and is plotted against the molar ratio of MINP to the substrate. The solid line is the best fit of the experimental data to the sequential binding of N equal and independent binding sites on the MINP. The heat of dilution for the substrate, obtained by adding the substrate to the buffer, was subtracted from the heat released during the binding. Binding parameters were auto-generated after curve fitting using Microcal Origin 7.

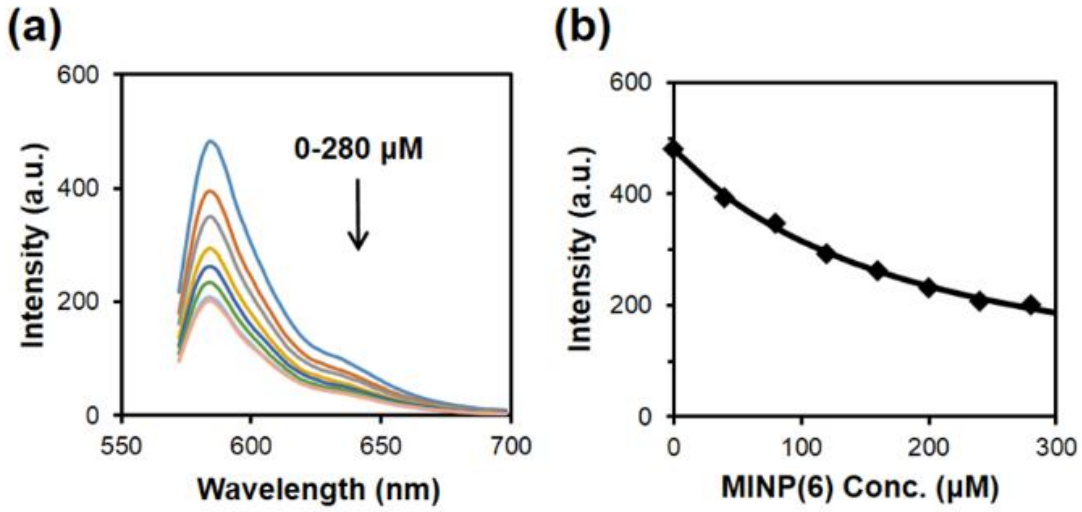

Figure S45. (a) Fluorescence spectra of reaction mixtures after 35 min at 37 °C in 10 mM HEPES buffer (pH7.4) in the Amplex Red assay. Each sample contained 30 µM Amplex Red reagent, 0.1 U/mL HRP, 2 U/ml of galactose oxidase, and 20 µM **1** dispersed in 1% POPC. (b) Nonlinear least squares curve fitting of the emission intensity at 585 nm to a 1:1 binding isotherm, yielding K_a = (5.42 ± 0.75) x 10^3 M^{-1}.

^{1}H NMR & ^{13}C NMR spectra

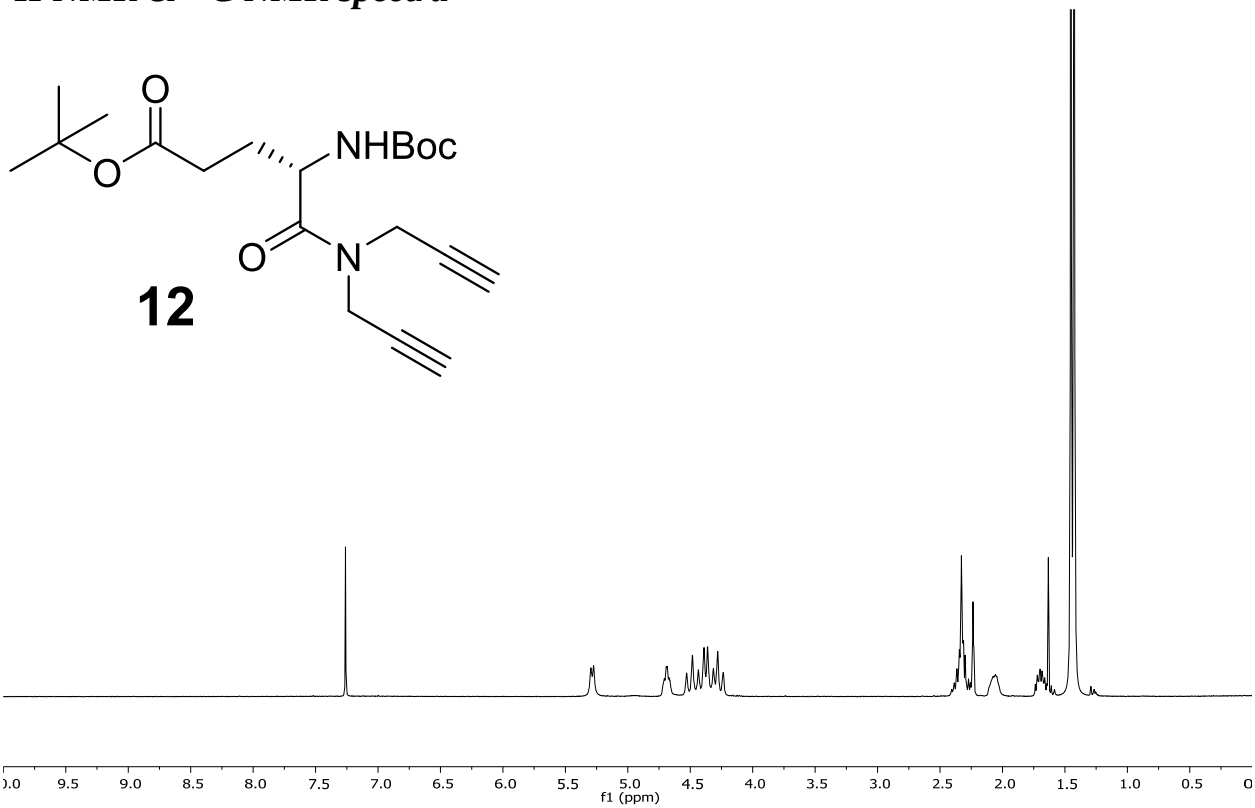

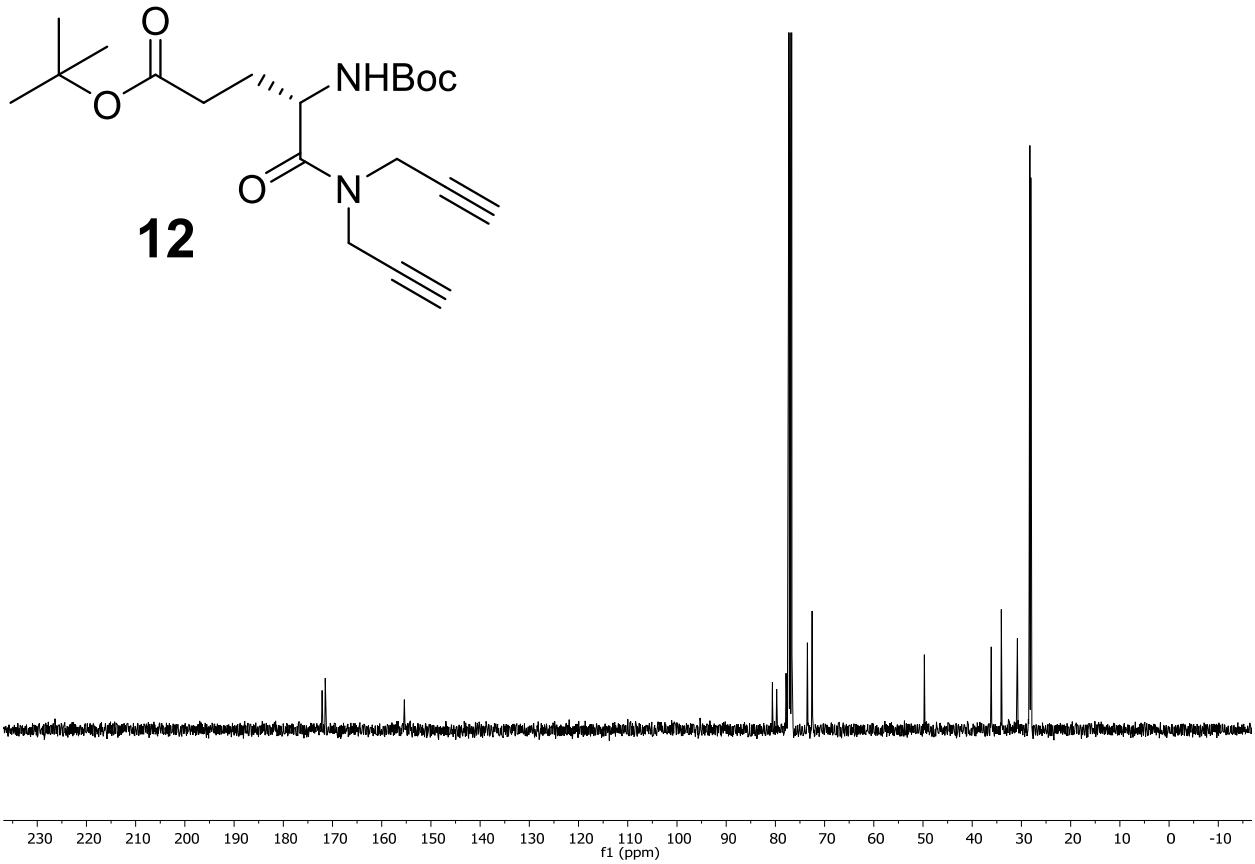

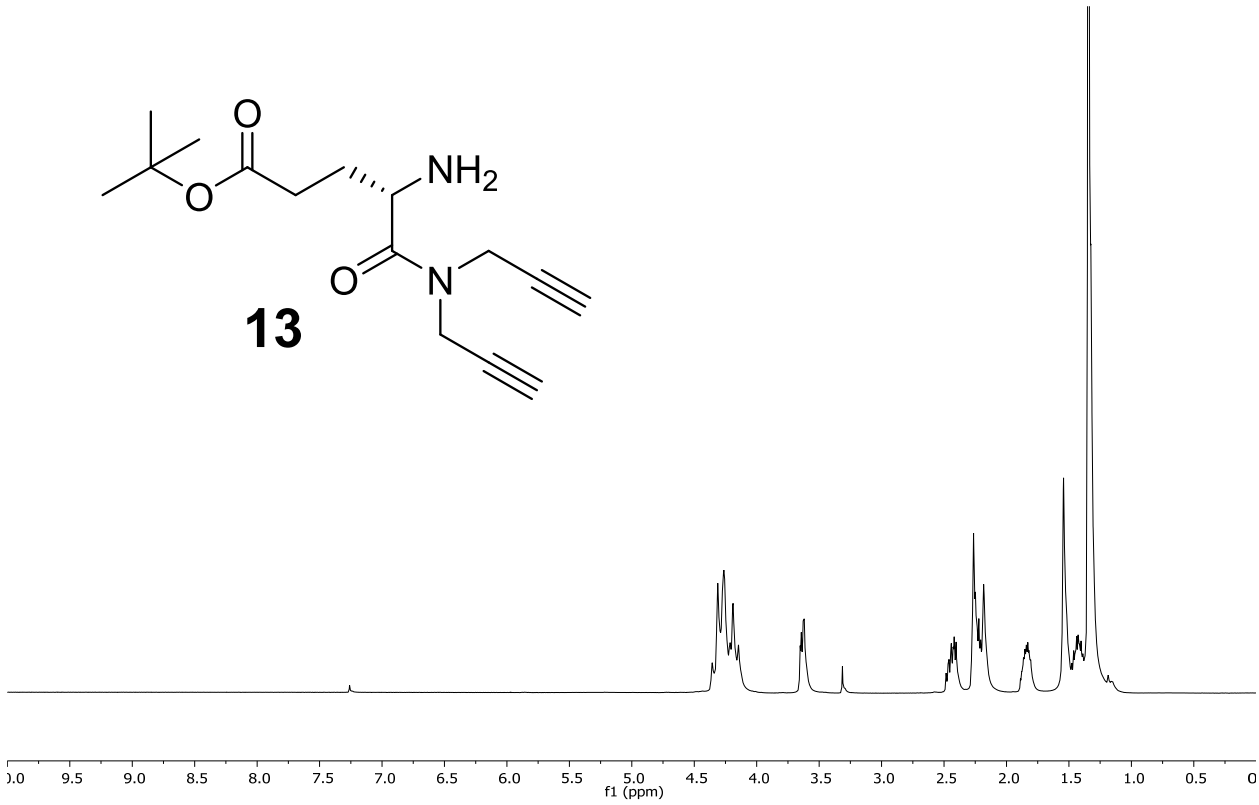
O
O
NH2
O
N
13
9.5
9.0
8.5
8.0
7.5
7.0
6.5
6.0
5.5
5.0
4.5
4.0
3.5
3.0
2.5
2.0
1.5
1.0
0.5
f1 (ppm)

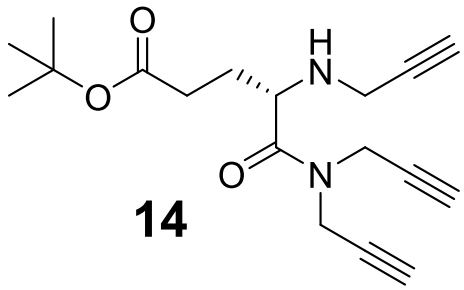
O
O
H
N
O
N

14

9.5
9.0
8.5
8.0
7.5
7.0
6.5
6.0
5.5
5.0
4.5
4.0
3.5
3.0
2.5
2.0
1.5
1.0
0.5
f1 (ppm)

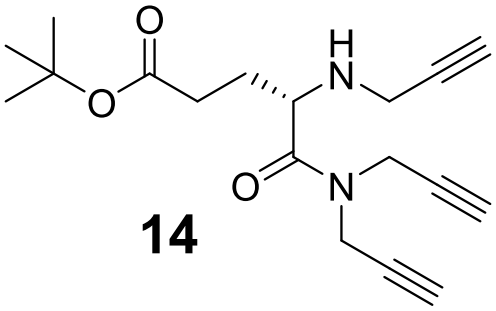
O
O
H
N
O
N

14

230
220
210
200
190
180
170
160
150
140
130
120
110
100
90
80
70
60
50
40
30
20
10
0
-10
f1 (ppm)

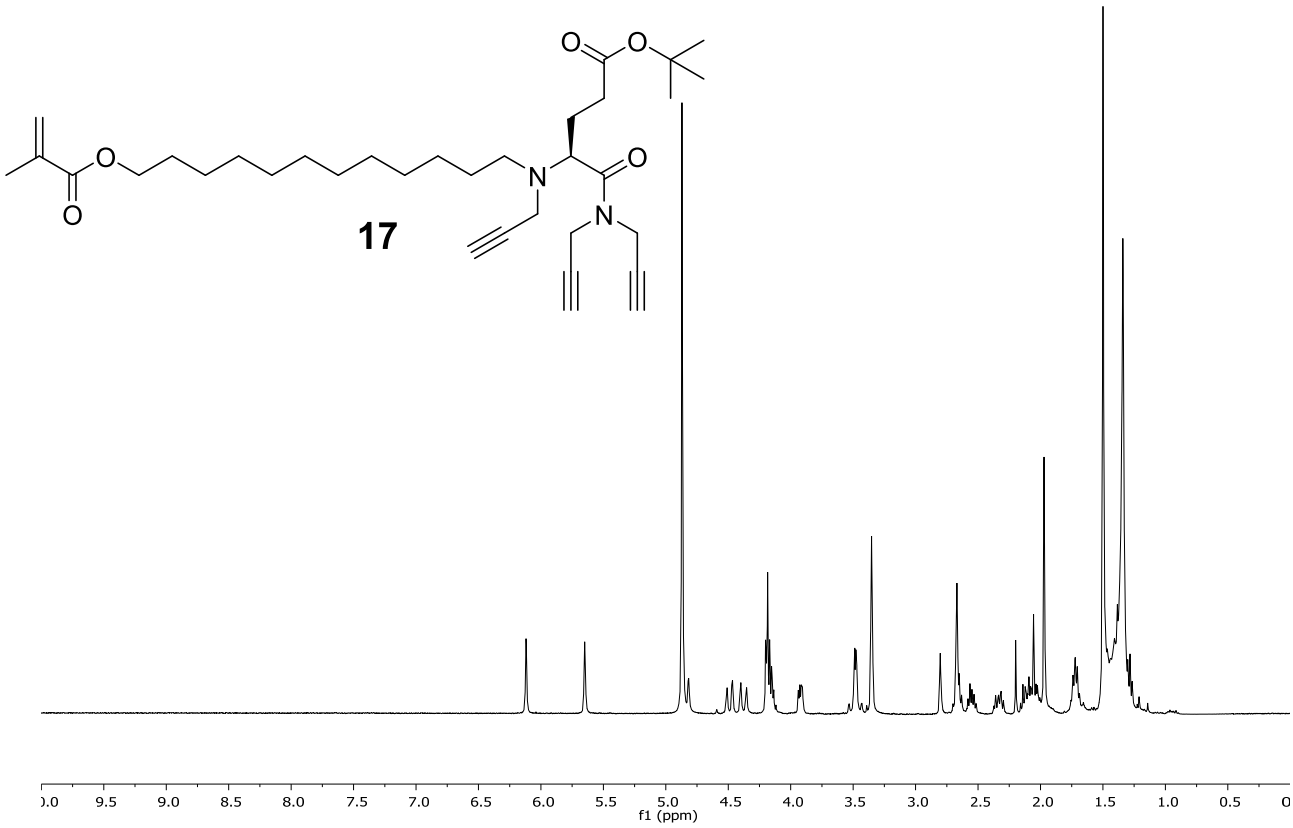
17
9.5 9.0 8.5 8.0 7.5 7.0 6.5 6.0 5.5 5.0 4.5 4.0 3.5 3.0 2.5 2.0 1.5 1.0 0.5
f1 (ppm)

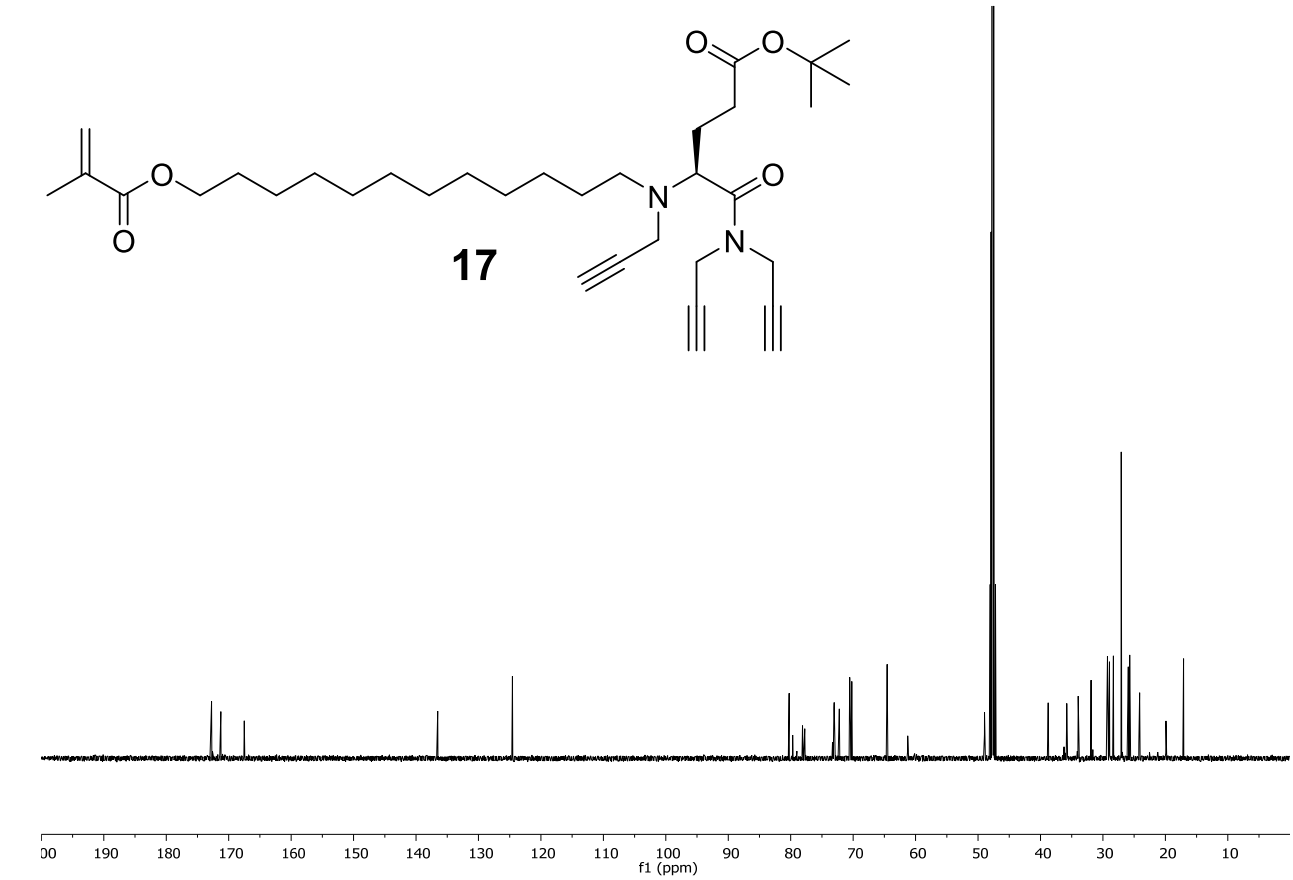
17
190 180 170 160 150 140 130 120 110 100 90 80 70 60 50 40 30 20 10
f1 (ppm)

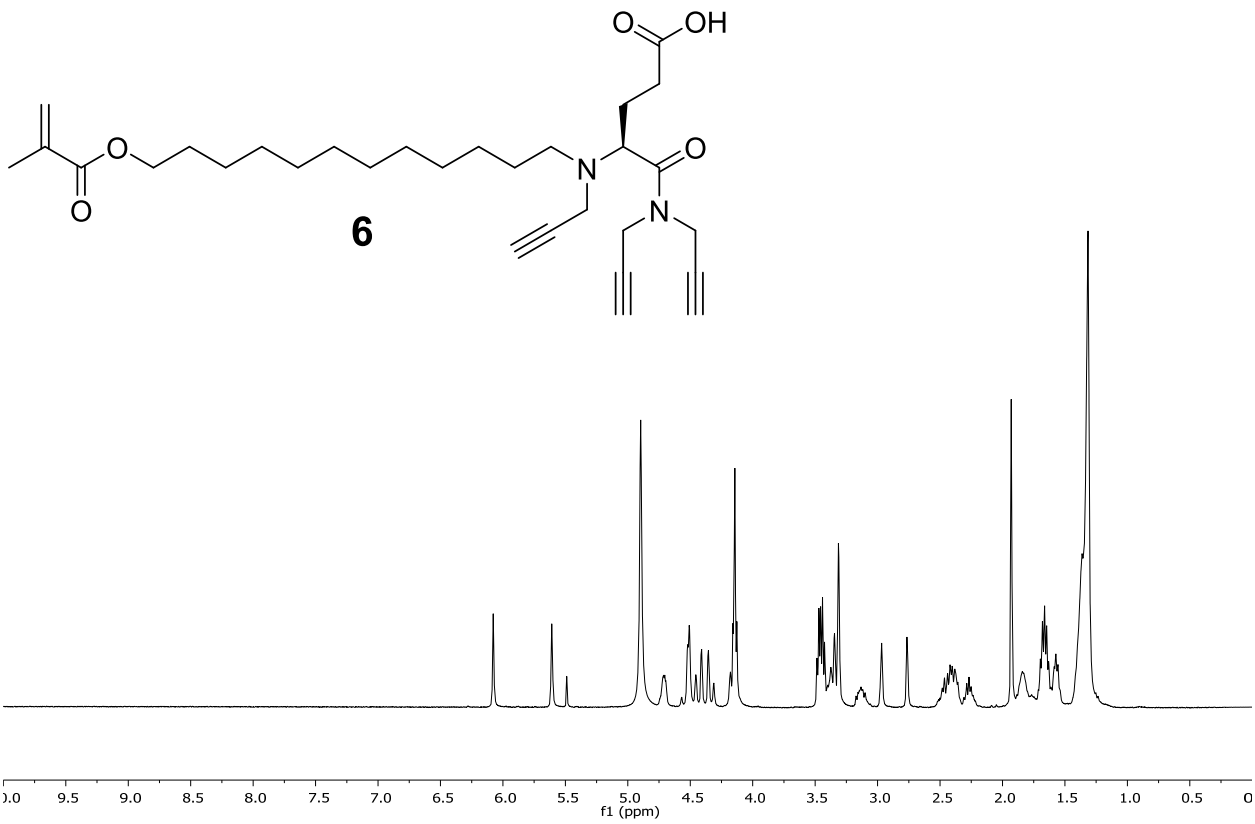
O
OH
O
O
N
O
N
6
9.5
9.0
8.5
8.0
7.5
7.0
6.5
6.0
5.5
5.0
4.5
4.0
3.5
3.0
2.5
2.0
1.5
1.0
0.5
f1 (ppm)

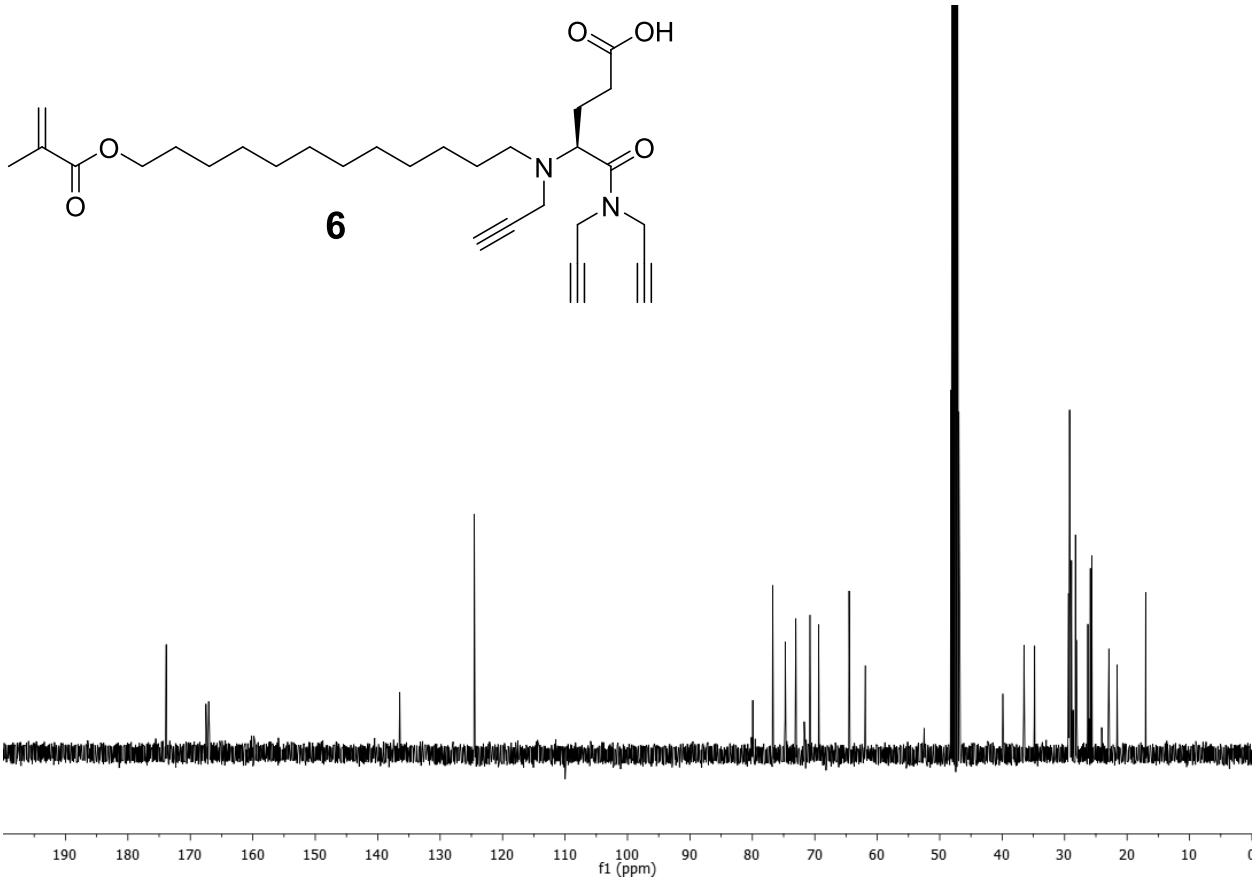
O
OH
O
O
N
O
N
6
190
180
170
160
150
140
130
120
110
100
90
80
70
60
50
40
30
20
10
f1 (ppm)